NPL REPORT
DQL RN004

Determination of the effective centres of the NPL long counters

Neil J Roberts, Hamid Tagziria, David J Thomas

NOT RESTRICTED

NOVEMBER 2004

Determination of the effective centres of the NPL long counters

Neil J Roberts, Hamid Tagziria*, David J Thomas
Quality of Life Division

* Presently at The European Commission, Joint Research Centre, IPSC, I-21020 ISPRA (VA), Italy
hamid.tagziria@jrc.it ; Tel: +39 0332 786324 Fax: +39 0332 785072

ABSTRACT
At the National Physical Laboratory, the standard instruments for measuring the neutron fluence of accelerator based neutron fields are long counters. This work follows on from an earlier project to derive improved knowledge of the response functions of the instruments using Monte Carlo calculations and measurements. In the present work new values for the effective centre as a function of energy have been calculated and validated experimentally. The efficiency values from the earlier work have been revisited in the light of new measurements and calculations. A sensitivity analysis has been performed to investigate the uncertainties in the calculated values. A final set of effective centre and efficiencies has been produced with realistic uncertainties for both the De Pangher and McTaggart type long counters.

ISSN 1744-0629

National Physical Laboratory
Hampton Road, Teddington, Middlesex, TW11 0LW

We gratefully acknowledge the financial support of the UK Department of Trade and Industry (National Measurement System Policy Unit)

Approved on behalf of the Managing Director, NPL
by Dr Desmond MacMahon,
authorised by the Director, Quality of Life Division

CONTENTS

1 INTRODUCTION

Long counters are the most popular flat response neutron detectors, i.e. detectors which have a relatively constant fluence response over a significant range of neutron energies. Their high efficiency, insensitivity to γ-rays, reasonable directionality, and good stability make them ideal for measuring neutron fluence over a wide range of energies. They are based on the use of a slow neutron detector (usually a BF_3 proportional counter tube) inside a cylindrical moderator which often includes an annulus of a thermal neutron absorber such as boron or cadmium to suppress the detection of neutrons incident from the side. They are typically about 50 cm in length and 22 cm in radius.

The National Physical Laboratory (NPL) has two types of long counter, shown in Figure 1:

- A De Pangher long counter designed by De Pangher and Nichols[De66] with a 38 mm outer diameter BF_3 tube. The one in use at NPL is one of a batch of six made by Centronic in the late 1960s[Ma70].
- A McTaggart type[Mc59], built at NPL, with a 50 mm outer diameter BF_3 tube for greater efficiency. From here on it will be referred to as the NPL long counter.

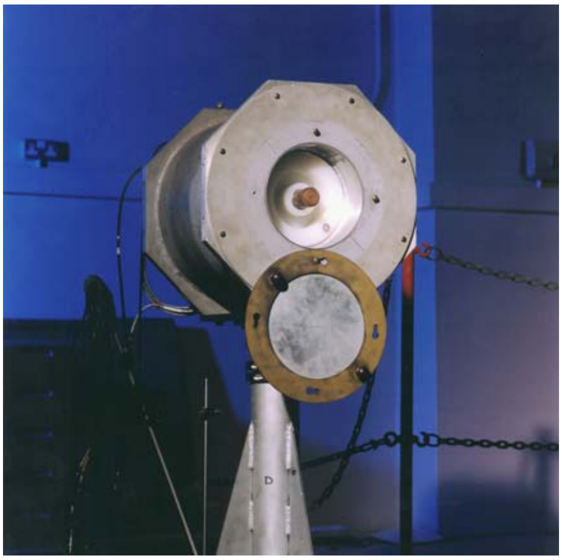


Figure 1: The De Pangher (shown with Cd cover displaced) and NPL long counters

Both long counters have non-equivalent front and back circular faces. The front (source-facing) faces are shown in Figure 1.

When making a fluence measurement with a long counter there are two parameters to consider:

1. Efficiency

   As they are neither 100% efficient nor perfectly flat in their response as a function of neutron energy, the efficiency has to be known for the energy or spectrum in which it is used.

2. Effective centre

   The effective centre of a device is the parameter, r_0, such that the count rate from a point source (either in vacuum or when allowance is made for scatter) falls off as $1/(r+r_0)^2$ with the distance, r, from the source to some convenient fixed point on the detector (usually the front face). Due to their cylindrical geometry and finite depth, the exact position of the effective centres of long counters is not obvious. The position varies with energy so the effective centre has to be determined for the particular energy spectrum in which it is used.

The values which have been in use up until recently for these two parameters for the two long counters at NPL came from a combination of measurements performed over 20 years ago by Hunt[Hu76] and empirical calculations using a formula based on available hydrogen and carbon cross section data (BNL325), as suggested by Allen[Al60].

Within the 1995 to 1998 National Measurement System programme at NPL, a project was set up to improve the data using new cross section values, improved source spectra, and more accurate calculations based on the Monte Carlo method[Ta98]. This yielded much improved values for the efficiency as a function of neutron energy which were validated experimentally, and cast doubt on the effective centre values given by Hunt. However, the determination of improved sets of effective centres required more work before the values of Hunt could be replaced with a high degree of confidence. As efficiencies and effective centres are closely related it is not sensible to use an efficiency from one evaluation with an effective centre from a different evaluation. The new efficiencies cannot therefore be introduced until new effective centres are also available.

The main objective of this work was thus to produce a set of reliable and justifiable effective centres, with appropriate uncertainties, for both the De Pangher and NPL long counters. This would be performed by reviewing previous measurements made with radionuclide sources and monoenergetic neutron beams, making new ones where required, and by carrying out Monte Carlo calculations of the effective centre for radionuclide source spectra and monoenergetic neutrons.

2 MONTE CARLO MODELLING

2.1 Introduction

An extensive set of Monte Carlo calculations for both detectors was carried out using MCNP-4B and later MCNP-4C[Br00]. For both long counters the geometries of the devices themselves were unchanged from those used in the earlier work[Ta98]. The models were constructed from engineering drawings supplied by Centronic (for the De Pangher counter) and by the NPL Engineering Services for the NPL long counter. In addition, the BF_3 tube of the De Pangher long counter was X-rayed to obtain, or confirm, details of the internal construction. Over 55 MCNP ‘surface’ cards and 35 ‘cell’ cards were used to describe the counters and their BF_3 tubes.

2.2 Initial method

Whereas the efficiency for a particular energy or spectrum can be calculated using a single MCNP run with a parallel neutron beam, it is not possible to calculate the effective centre in this way. The method used here involved calculating the decrease in response with distance, r, from a point source then fitting a function of the form $1/(r+r_0)^2$ to yield the effective centre, r_0. Each different distance was handled by a new MCNP run. This is very similar to the method used when making a measurement of the effective centre, but with the advantage that the need for a scatter correction is eliminated by modelling the long counter in a vacuum with no scattering material such as walls, floor, or ceiling present.

To improve on the convergence of the calculation, the model uses a point source with the SB source biasing card. This enables more particles to be emitted in the direction of interest by reducing their weight, thereby keeping the total weight of emitted particles isotropic. The direction cosine, μ, of the source emission was sampled from an exponential function [$p(\mu)=ce^{a\mu}$] with a=3.5. The same value of a was used for all distances which meant that the biasing was more pronounced for the nearer distances. A feature of MCNP is that for each distance, the emitted neutrons will, by default, leave the source with the same sequence of directions and energies. This correlation may or may not be welcome.

For each energy, 50 calculations were made with the source on the axis of the long counter but at different distances from the front face of the counter, ranging from 115 to 600 cm. The De Pangher and NPL long counter models were run for 10^7 histories from 115 to 200 cm, 1.5×10^7 from 205 to 300 cm, 2×10^7 from 310 to 400 cm, and 3×10^7 from 420 to 600 cm. The $1/r^2$ decrease in the fluence with distance r can then be used to identify the exact position inside the long counter at which it behaves as a point detector.

Details of the analysis procedure were given in references [Ta98] and [Ta01] and thus only the essentials will be repeated here for completeness.

For a point detector and a point source in vacuum one can write that:

$$Cr^2 = \text{Constant} \qquad (1)$$

where C is the detector count rate and r is the source to counter distance.

Allowing for scatter and geometry effects, a corresponding expression for a long counter has been suggested by Hunt[Hu76][Hu80][IS00] and is given by:

$$[C_t(r) - C_i(r)]F_a(r) = \frac{K}{(r+r_o)^2} \qquad (2)$$

where

$C_t(r)$ and $C_i(r)$ are total and in-scatter measured count rates at a source to detector distance r measured to the front face of the counter moderator.

$F_a(r)$ is the air out-scatter correction factor (derived from the oxygen and nitrogen cross sections),

r_0 is the effective centre distance into the moderator front face (i.e. a positive value means that the effective centre is within the counter and further from the source than the moderator front face which is effectively used as a reference surface for source to counter distance)

and K is the source-detector characteristic constant.

Rearranging the above expression gives:

$$1\Big/\sqrt{[C_t(r) - C_i(r)]F_a(r)} = \frac{1}{\sqrt{K}}(r + r_o) \tag{3}$$

and it follows that r_0 and K can be obtained by a least squares fit, i.e.,

$$1\Big/\sqrt{[C_t(r) - C_i(r)]F_a(r)} \quad \text{against} \quad r \tag{4}$$

with the gradient equal to $\frac{1}{\sqrt{K}}$ and the intercept equal to $\frac{1}{\sqrt{K}} r_o$. (5)

Subsequently, the efficiency ε can be evaluated by

$$\varepsilon = \frac{4\pi K}{QF_I} \tag{6}$$

where Q is the source strength, i.e., the total emission rate into 4π steradians, and F_I is the anisotropy factor of the radionuclide source.

2.2.1 De Pangher long counter

The MCNP geometry of Tagziria[Ta98] for the De Pangher long counter is shown in Figure 2.

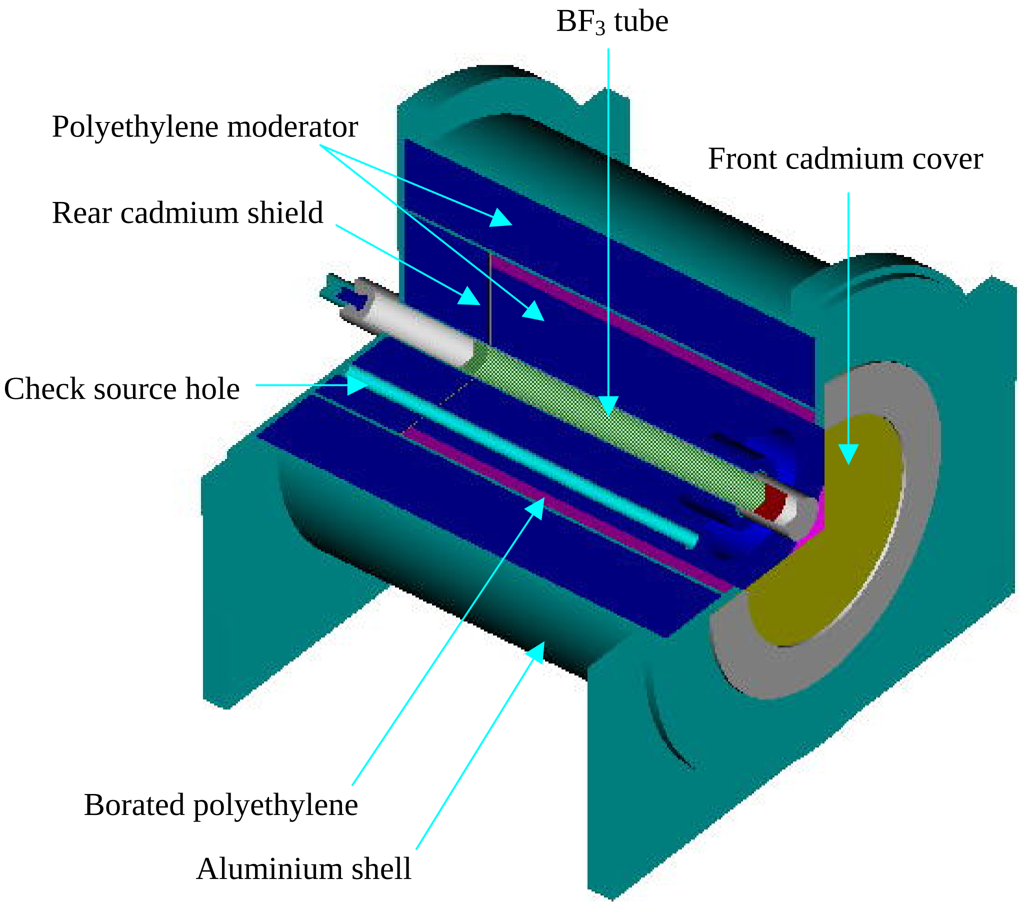

Figure 2: The MCNP model of the De Pangher long counter with section removed

The effective centre was calculated for 145 energies from 0.01 to 6 MeV. The results are plotted in Figure 3 alongside the previously used empirical fit of Hunt. The MCNP results show a large amount of fine structure, with the effective centre changing by as much as 5 cm for a change in energy of only 150 keV. If the structure is ignored, the same trend of the effective centre moving further into the long counter with increasing energy is apparent. A simplistic explanation of this effect is that higher energy neutrons need more collisions to thermalise and hence they travel further into the long counter before being captured in the BF_3 tube.

For almost all energies the MCNP calculation gave an effective centre closer to the front face of the long counter when compared with the fit of Hunt.

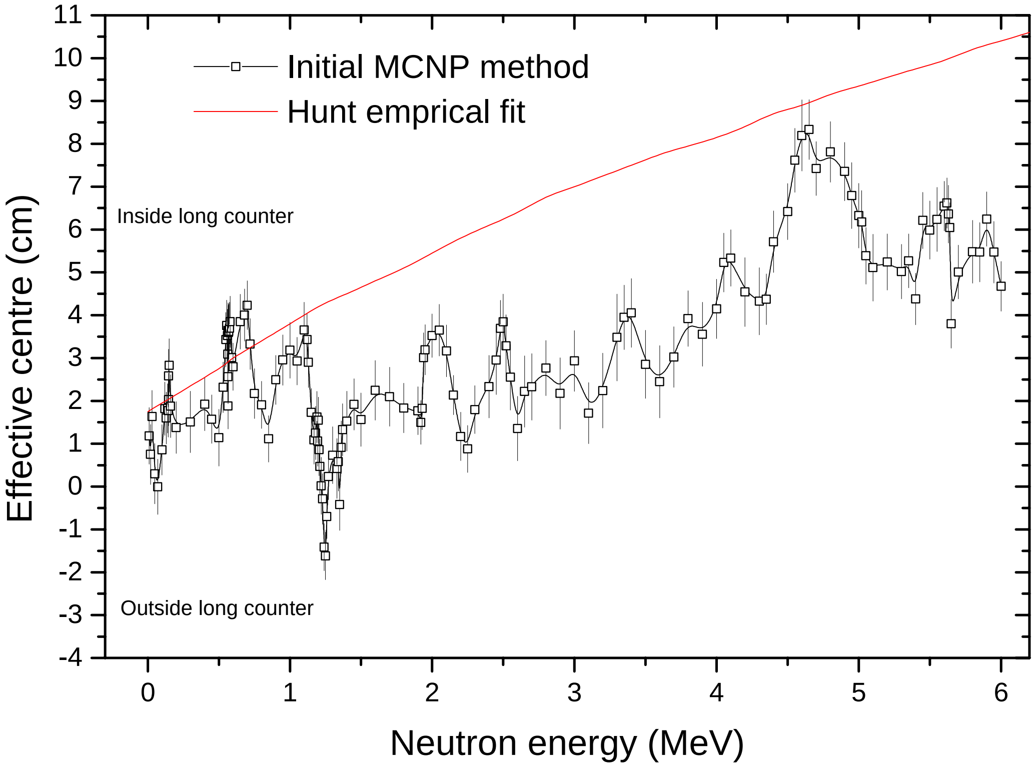

Figure 3: Initial MCNP calculated effective centres for the De Pangher long counter shown with the Hunt empirical fit (line connecting MCNP points intended as a guide only)

2.2.2 NPL long counter

The MCNP geometry of Tagziria[Ta98] for the NPL long counter is shown in Figure 4.

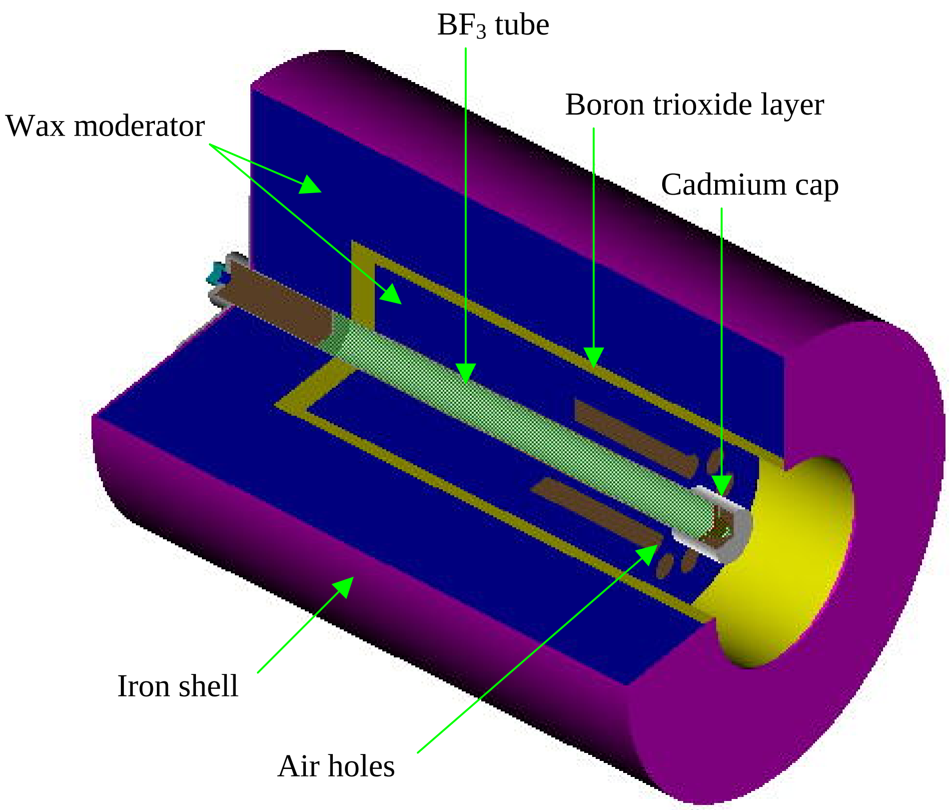

Figure 4: The MCNP model of the NPL long counter with section removed

The effective centre was calculated for 145 energies from 0.001 to 6 MeV. The results are plotted in Figure 5 alongside the previously used empirical fit of Hunt. As with the De Pangher results, the MCNP calculations of effective centre show a lot of structure but the same overall trend of moving further into the long counter as the energy increases. The MCNP values are lower than those of Hunt, particularly at higher energies where the difference can be as much as 5 cm. For a measurement at a source to long counter distance of 2 m, a typical distance used at NPL, a 5 cm error in the effective centre would correspond to a 5% error in the measured fluence.

The extensive fine structure of the MCNP calculated effective centres and the large changes in value with relatively small changes of neutron energy were not expected. No mechanism for producing this structure could be identified, particularly as the structure bore no relation to structures in the cross sections of the constructional materials of the long counters. (Structure in the efficiency as a function of energy can be correlated exactly with structures in the cross section of carbon – a major constituent of the moderating material.) It was therefore felt that some further investigation of the calculated results was warranted.

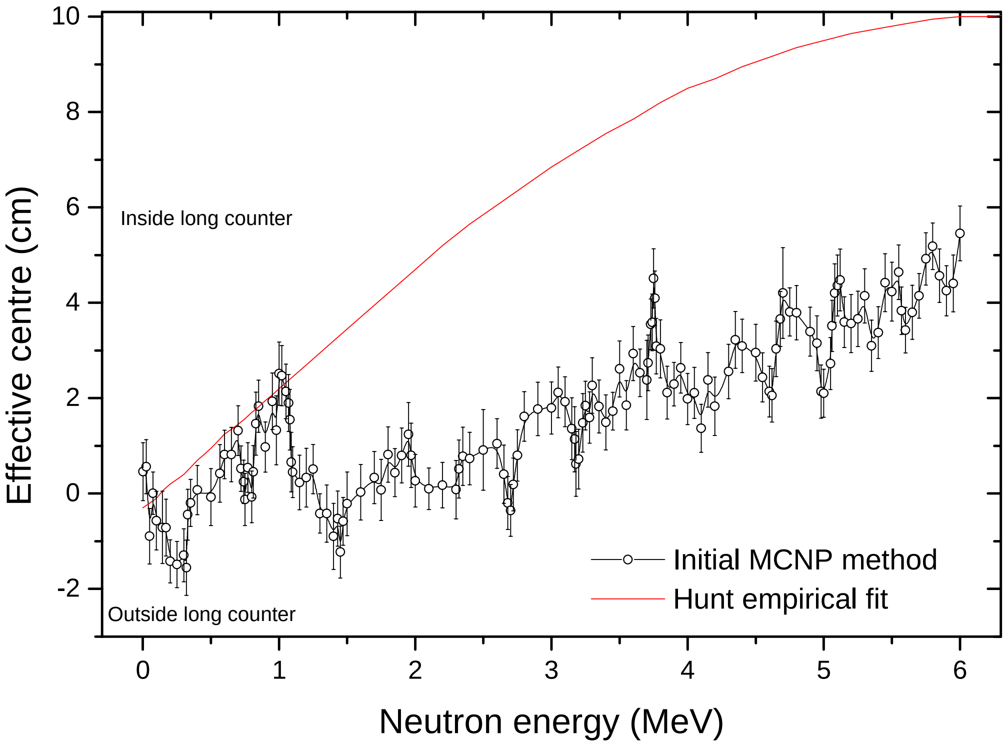

Figure 5: Initial MCNP calculated effective centres for the NPL long counter shown with the Hunt empirical fit (line connecting MCNP points intended as a guide only)

2.3 Random number method

2.3.1 The case of two monoenergetic neutron beams

To test for consistency, a spectrum consisting of two monoenergetic neutron components (1.1 and 1.25 MeV) with equal probability was used as the input to the De Pangher model. These two energies were chosen because of the large difference in calculated effective centres despite their comparative closeness in energy. The effective centre result was then compared with the values for each energy individually. The effective centre of the two combined should equal the mean of the two individual effective centres.

The results in Table 1 show that the combined spectrum gives a much larger value for the position of the effective centre than taking the mean of the two individual values. The combined value is in fact higher than either of the individual values. This is a clear inconsistency in the model, and it would be very difficult to think of any explanation for why the combined effective centre of two energies could be so different from the mean of the individual effective centres.

Table 1: De Pangher effective centre values for two monoenergetics individually and combined

Neutron spectrum (MeV)	Effective centre (cm)
1.10	3.65 ± 0.65
1.25	-1.62 ± 0.56
Mean of 1.10 and 1.25	1.02 ± 0.43
Combined 1.10 and 1.25	4.56 ± 0.79

Correlations between the calculations at each source to long counter distance for a given energy were suspected as a possible cause of the inconsistency. MCNP uses correlated sampling whereby the *i*th history in one run uses the same initial pseudorandom number as the *i*th history in another run. The histories themselves may then diverge due to differences in the model, but the (*i*+1)th histories again begin with the same initial number. In the case of the effective centre calculations, this leads to the neutrons in each run being emitted from the source with the same angles. For adjacent source to long counter distances this will result in the neutrons being incident on almost the same positions on the front face. This could cause problems when combined with the non-uniformity of response across the front face.

To remove any correlations due to using the same starting pseudorandom number for each distance, a different random starting number for each distance was chosen randomly. To overcome any problems associated with source biasing, the biasing was replaced by defining the source to only emit neutrons in the cone subtended by the long counter. The tally results were normalised using a solid angle correction factor. Six runs were performed for 1.1, 1.25 and 1.1+1.25 MeV. Results are shown in Figure 6. The graph demonstrates that, using this approach, the mean of the 2 effective centres (1.1 and 1.25 MeV) agrees with the mean effective centre of a spectrum consisting of 50% 1.1 MeV and 50% 1.25 MeV. Note that due to the removal of source biasing the default starting number values in the graph are different to those in Table 1.

The graph also shows how different the effective centre is when calculated using the default starting number. For each case it is outside the range of the points calculated using different random starting numbers.

The difference in effective centres that can be achieved just by using different starting random numbers is remarkable. For 1.25 MeV, the highest and lowest are 1.5 cm apart. This emphasises the need to perform several calculations at each energy to average out extreme cases. A possible explanation is that the illumination of the long counter at each distance is insufficiently uniform (i.e. the more sensitive regions sometimes receive an unbalanced share of neutrons which skews the tally at that distance). The shift at a particular distance would probably be within the uncertainties for a fluence measurement, but could perhaps be sufficiently large to alter something as sensitive as the effective centre.

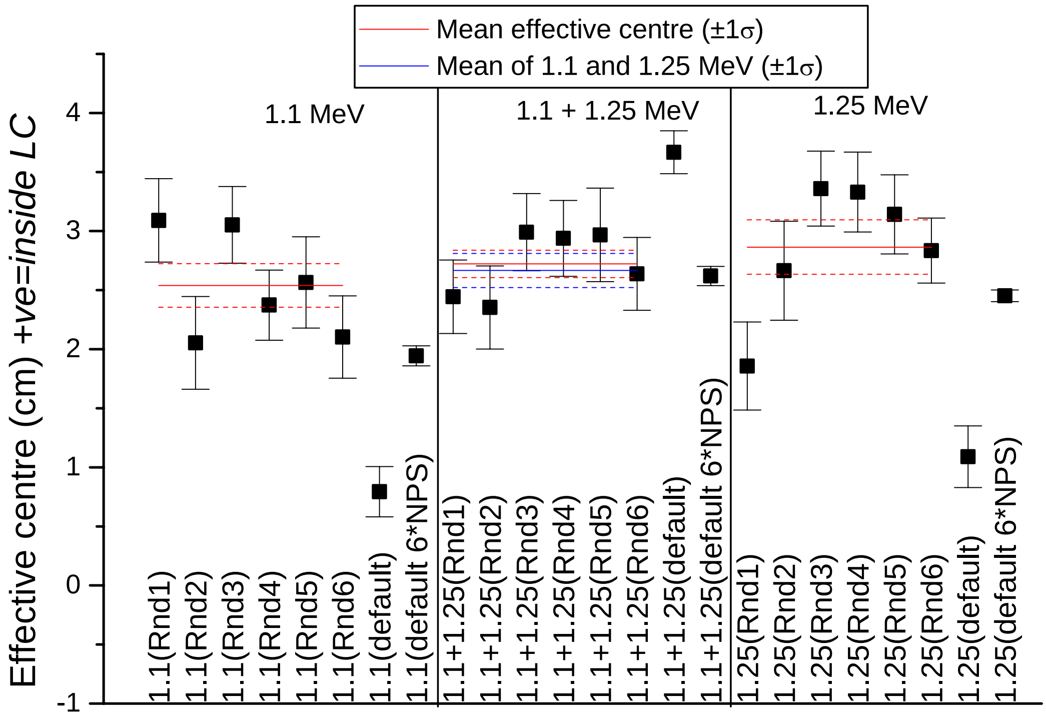

Figure 6: Effective centres of 2 monoenergetics, independently and together

Also shown in Figure 6 are the values obtained by running for 6 times the number of particles (NPS) with the default random starting number for each distance. For each energy this changed the effective centre by far more than the uncertainty, demonstrating that either the uncertainties were too small, or that a convergence problem exists. Whilst running for longer at each distance does improve the agreement, the mean of the two individual values still does not equal the value from the combined spectrum within the uncertainties. It therefore appears to be better to so separate runs with different initial random numbers (and this is what was done in the present work), even though one might expect a single long run of the same total number of histories to be equivalent. Five runs are satisfactory to yield a reliable mean value.

2.3.2 Description of method

The important features of the new method are as follows:

1. The DBCN card is used to change the default starting pseudorandom number. A Visual Basic program is used to generate the input files for a particular run, and its own internal random number generator selects a number up to 13^8, having been reinitialised each time. The value of 13^8 has no special significance, it was fixed upon only because it was found to give satisfactory numbers for the DBCN card. As the starting pseudorandom number in MCNP cannot be even, the program checks for this and adds 1 if necessary.

2. The DIR option is used with the SDEF card to restrict the direction of emitted neutrons to a cone subtended by the entire front face of the long counter. An SI card is used to give the direction cosine histogram which is calculated by the Visual Basic program. The histogram consists of only two points: the direction cosine of the edge of the cone, and 1. An SP card is used to give the probability distribution of “0 1”. This maximises the efficiency of the calculation by ensuring that no neutrons miss the front face of the long counter completely, and it also removes any doubts about the effect of changing the weight of particles as a function of angle. The Visual Basic program adds in a component to the FM tally multiplier to compensate for the reduction in solid angle for each distance, and hence give an answer in terms of an isotropic source emitting into 4π steradians.

3. Five separate runs, each consisting of 50 distances from 115 to 600 cm, are performed all with different starting pseudorandom numbers. At each distance the mean is taken, and the standard error is calculated from the spread of the results. This washes out any rogue answers that seem to arise when a particular set of starting pseudorandom numbers are chosen for a particular run. The number of histories is the same for each distance; 10^6 for the De Pangher, and 5×10^5 for the NPL long counter. The data are analysed using the same least squares fitting procedure as described earlier.

2.3.3 De Pangher long counter results

The density of the BF_3 gas in the model was increased by 4%, from that used by Tagziria[Ta98], to normalise the efficiency with measurements. This was based on the value of efficiency from a measurement made by Tagziria for ^{252}Cf[Ta98]. Although further normalisation by a smaller amount will be required later, it was considered better to change the model at this stage in case the gas pressure had an influence on the effective centre. The cylindrical hole for a check source that was previously filled with air was changed to be filled with polyethylene as measurements are always made with a dummy check source rod inserted.

As the new method requires 5 times the number of histories as the initial method to calculate an effective centre, the choice of energies to investigate had to be more selective. Points were chosen either because they corresponded to energies where the initial method indicated that the effective centre had structure, or because the profile of efficiency versus energy had a peak or a trough at that point.

The effective centre was calculated for 51 energies between 0.001 and 6 MeV, as well as for ^{124}Sb-Be, ^{252}Cf, and ^{241}Am-Be energy spectra, as shown in Figure 7. The graph shows that the new method produces far less structure than the initial method. The sharp changes that are present match with features in the efficiency profile, and these in turn match with structure and resonances in the carbon cross-section (Figure 9). Sharp resonances cause a drop in the efficiency and also move the effective centre towards the front of the long counter.

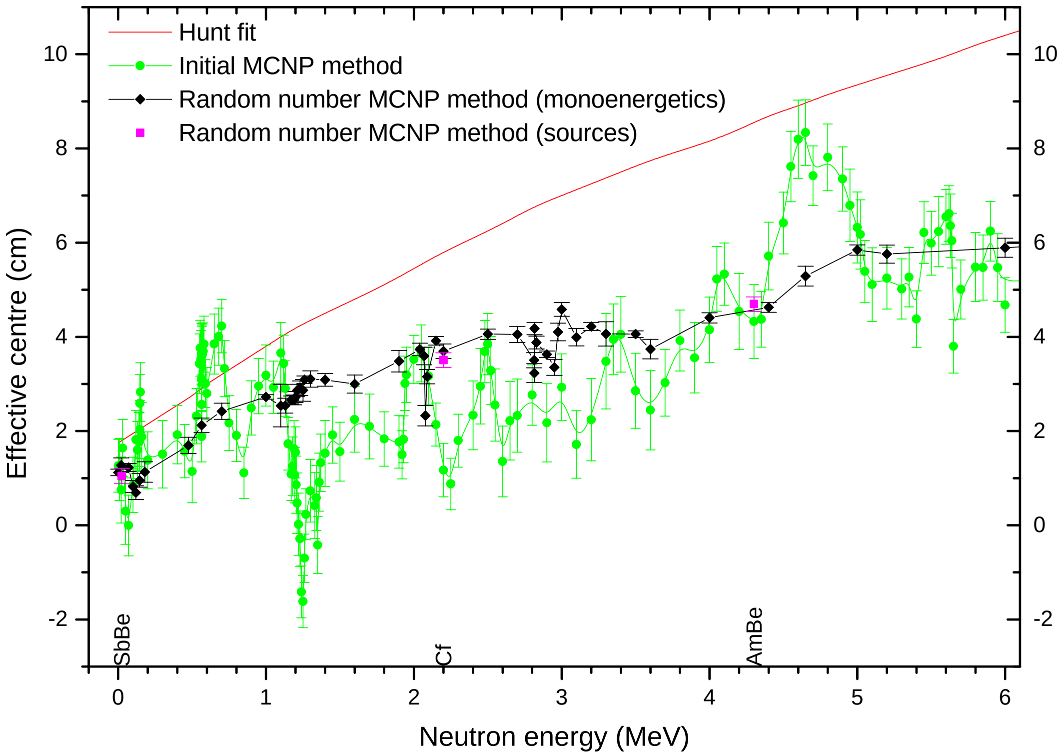

Figure 7: Comparing random number method calculated De Pangher effective centres with previous calculations (line connecting MCNP points intended as a guide only)

The efficiency calculations of Tagzirìa[Ta98] used a parallel beam source which enabled the value at each energy to be calculated in a single run. The point source method used in the present work to determine effective centres also yields values for the efficiency (equation 6). The two sets of values are plotted in Figure 8. The agreement is very good with the exception of the energy range from 0.3 to 1.0 MeV where the parallel beam method indicates a peak at 0.475 MeV and a trough at 0.7 MeV, but the point source method shows a smooth variation over the range. The overall agreement verifies the use of a parallel beam to calculate the efficiency, and it demonstrates the consistency of the model.

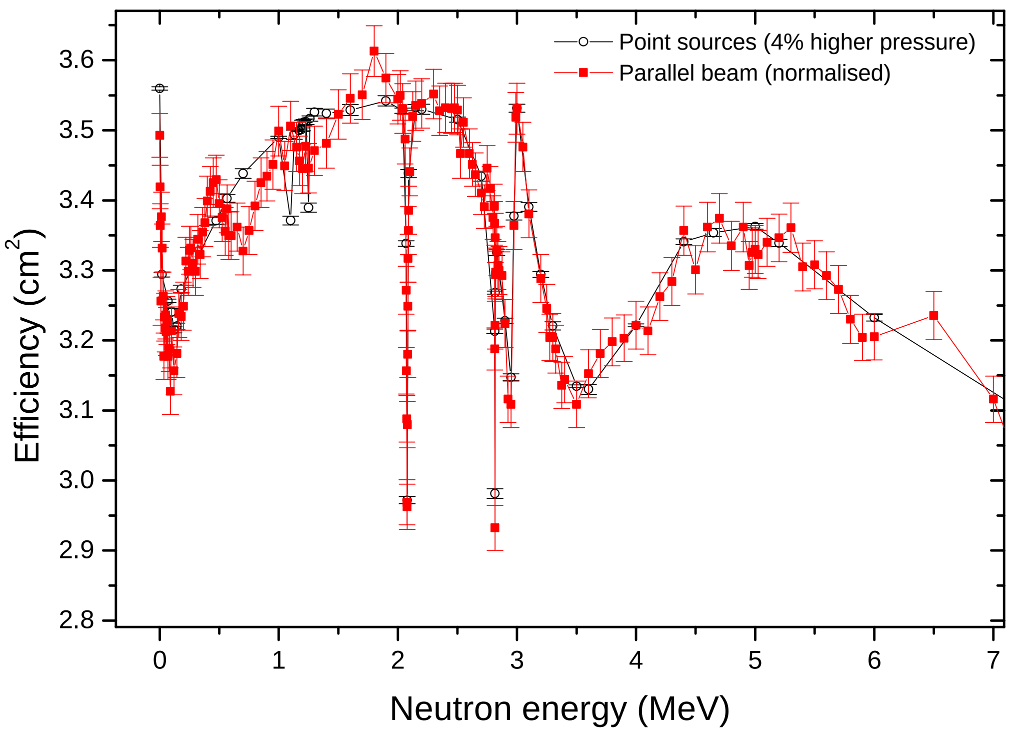

Figure 8: Comparison of De Pangher efficiencies calculated using a parallel beam and with point sources (line connecting MCNP points intended as a guide only)

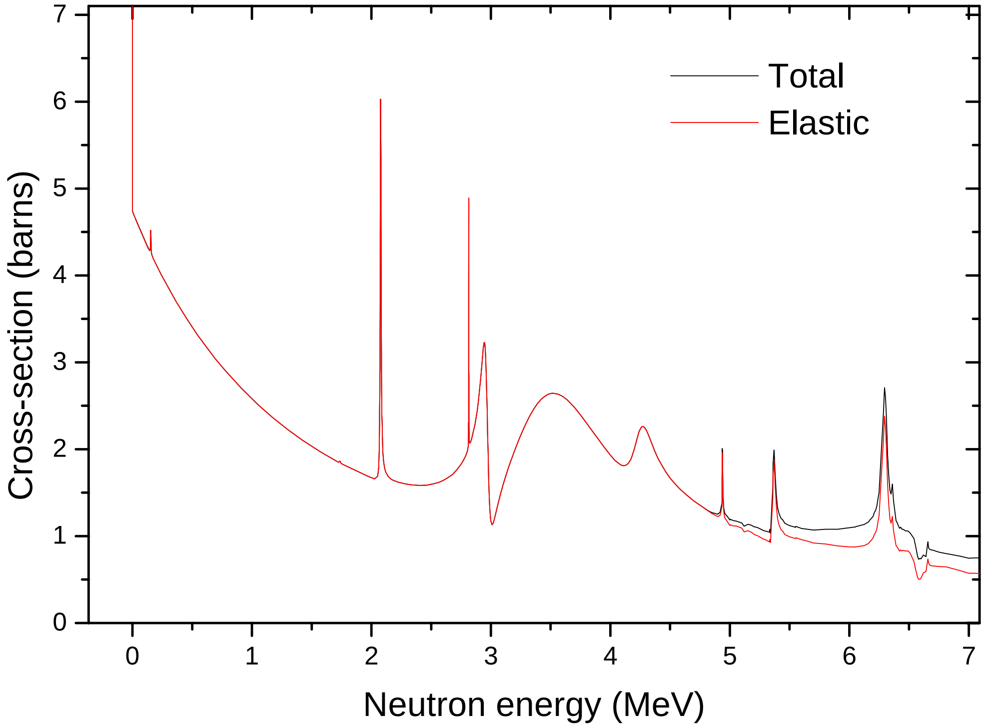

Figure 9: ENDF/B-VI neutron interaction cross-sections for natural carbon

2.3.4 NPL long counter results

No changes were made to the density of the BF_3 gas in the NPL long counter model of Tagziria[Ta98] to improve agreement of the efficiency with measurement. Small changes in the gas pressure are unlikely to change the effective centre.

The effective centre was calculated for 42 energies between 0.03 and 6 MeV as shown in Figure 10. As with the De Pangher, the new method produces far less structure than the initial method. For the NPL long counter the sharp changes that are present also match with features in the efficiency profile and hence the carbon cross-section.

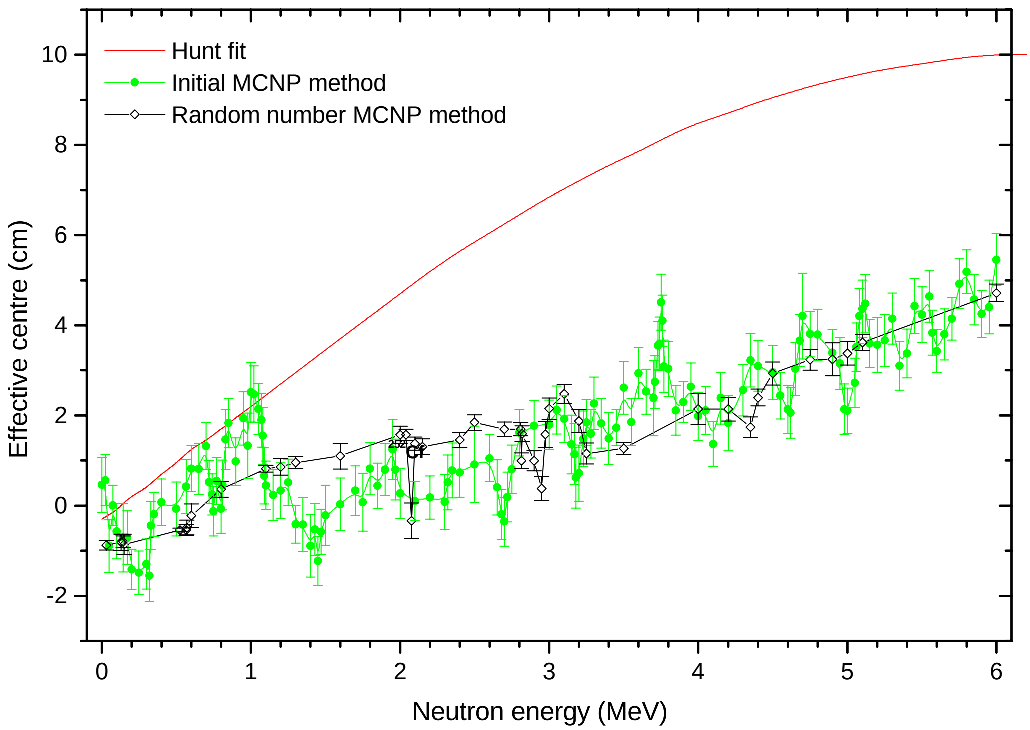

Figure 10: Comparing random number method NPL long counter calculated effective centres with previous calculations (line connecting MCNP points intended as a guide only)

The values of efficiency calculated from the point source calculations are compared with those from a parallel beam[Ta98] in Figure 11. There is excellent agreement for all energies which verifies the parallel beam approach, and shows consistency in the model.

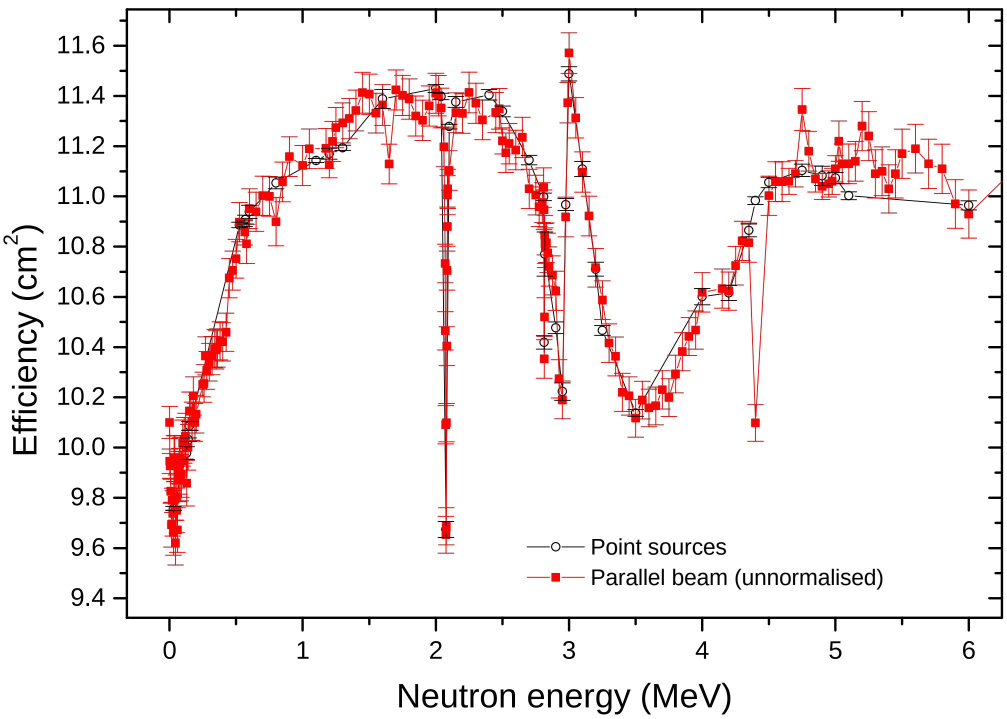

Figure 11: Comparison of NPL long counter efficiencies calculated using a parallel beam and with point sources (line connecting MCNP points intended as a guide only)

2.3.5 Sensitivity analysis

Any Monte Carlo calculation is only as good as the input data given to it, regardless of the statistical uncertainty in the final answer. The geometry of the problem, the densities of materials, and the cross-section data all have some uncertainty associated with them. It is therefore important to study the sensitivity of the results to realistic changes in the input data. To include all materials, all cells, and all cross-sections in the sensitivity analysis would be an onerous task, with most having little or no effect on the results. Therefore the parameters to investigate were chosen on the basis of those most likely to have an effect on the final answer, and those that are least well known.

The NPL long counter model has been used for the sensitivity analysis as it is more efficient than the De Pangher model. All parameters investigated for the NPL long counter will also be applicable to the De Pangher with the exception of the moderator composition, where polyethylene, with a well-defined composition, is used instead of wax.

As effective centres are calculated by plotting the results from 50 runs, the application of the PERT card in MCNP to calculate the change in the effective centre due to a change in the model would not be straightforward. In any case the PERT card cannot be used to study changes in the physical geometry of the model, or changes in the cross-sections. The simpler approach used here was to perform new calculations with the amended model, and look for differences in the effective centre greater than the statistical uncertainty from the spread of the 5 random number MCNP runs. However, the PERT card was used to calculate the change in efficiency due to changes in the moderator density and composition.

An attempt to investigate the sensitivity of the results to the method used was also made by using a different number of source to long counter distances to determine the effective centre.

2.3.5.1 Moderator density

The density of the wax in the model of the NPL long counter was increased from 0.92 to 0.94 g cm^{-3}. Random number method effective centre and parallel beam efficiency MCNP calculations were performed for 0.144, 1.2, and 5.0 MeV. The changes in the effective centre and efficiency are given in Table 2. The PERT card gives the change in efficiency together with the statistical uncertainty in the change. For the parallel beam calculations the uncertainty in the change is given in Table 2 instead of the uncertainty in the perturbed efficiency.

Table 2: Changes in the effective centre and efficiency of the NPL long counter with a change in wax density

	144 keV			1.2 MeV			5.0 MeV		
Density (g.cm^{-3})	0.92	0.94	Change	0.92	0.94	Change	0.92	0.94	Change
Effective centre (cm)	-0.80 ± 0.13	-1.08 ± 0.27	-0.28	0.86 ± 0.19	0.85 ± 0.19	-0.01	3.38 ± 0.26	3.14 ± 0.16	-0.24
Efficiency (cm^2)	10.078 ± 0.093	9.990	-0.088 ± 0.017	11.215 ± 0.099	11.135	-0.080 ± 0.019	11.132 ± 0.097	11.077	-0.055 ± 0.020

For each energy, the change in effective centre was within the statistical uncertainty so it can be concluded that it is insensitive to a change in the wax density of this proportion. At the higher density, the efficiencies did decrease by more than the uncertainties in the changes. However the changes were still within the statistical uncertainties in the original efficiency values.

2.3.5.2 Moderator composition

In the model of Tagziria for the NPL long counter, the composition of the wax is approximated as CH_2. Data from the NIST website[NI] indicates that the composition could be 14.8605% hydrogen, and 85.1395% carbon by weight (equivalent to $CH_{2.08}$). Random number method effective centre and parallel beam efficiency MCNP calculations were performed for 0.144, 1.2, and 5.0 MeV. The changes in the effective centre and efficiency are given in Table 3 and can be seen to be negligible within the uncertainties.

Table 3: Changes in the effective centre and efficiency of the NPL long counter with a change in wax composition

	144 keV			1.2 MeV			5.0 MeV		
Composition	CH_2	NIST	Change	CH_2	NIST	Change	CH_2	NIST	Change
Effective centre (cm)	-0.80 ± 0.13	-0.89 ± 0.18	-0.09	0.86 ± 0.19	0.90 ± 0.07	+0.04	3.38 ± 0.26	3.32 ± 0.15	-0.06
Efficiency (cm^2)	10.078 ± 0.093	10.067	-0.011 ± 0.011	11.215 ± 0.099	11.208	-0.007 ± 0.007	11.132 ± 0.097	10.067	0.030 ± 0.013

2.3.5.3 Hole radius

The radius of the 8 holes in the front face of the moderator of the NPL long counter was increased from 1.27 to 1.32 cm. Random number method effective centre and parallel beam efficiency MCNP calculations were performed for 0.144, 1.2, and 5.0 MeV. The changes in the effective centre and efficiency are given in Table 4.

Table 4: Changes in the effective centre and efficiency of the NPL long counter with a change in the radius of the holes in the front face of the moderator

	144 keV			1.2 MeV			5.0 MeV		
Hole radius	1.27 cm	1.32 cm	Change	1.27 cm	1.32 cm	Change	1.27 cm	1.32 cm	Change
Effective centre (cm)	-0.80 ± 0.13	-0.72 ± 0.26	+0.08	0.86 ± 0.19	0.95 ± 0.18	+0.09	3.38 ± 0.26	3.67 ± 0.18	+0.29
Efficiency (cm^2)	10.078 ± 0.093	10.312 ± 0.093	+0.234	11.215 ± 0.099	11.383 ± 0.099	+0.168	11.132 ± 0.097	11.160 ± 0.097	+0.028

The changes in the effective centre are all within the statistical uncertainties so it can be said that the effective centre is insensitive to small changes in the radius of the 8 holes in the front of the moderator.

The efficiency does show a definite increase as the radius increases for 144 keV and 1.2 MeV, but not for 5 MeV. This can be explained using the radial efficiency plot shown later in Figure 14. The air ring in the De Pangher is analogous to the air holes in the NPL long counter and the graph shows that for energies of 1.2 MeV and below the air ring is by far the most efficient region of the front face. The diameter of the holes in the NPL long counter corresponds to 1 inch, and measurements indicate that a radius of 1.32 cm is unrealistically large so the changes shown in the table are overestimated.

2.3.5.4 Cross-section data

As the PERT card cannot be used to make small changes to the cross section data, it is necessary to use data from older evaluations in order to investigate the sensitivity of the results. The newer evaluations should be better and more reliable than the older evaluations, so the results obtained using the older cross section values represent the maximum likely change due to uncertainties in the evaluated data. The sources of the MCNP-4C default cross-sections and the older values are given in Table 5.

Table 5: Sources of cross section data

Element / isotope	MCNP-4C default		Old	
	ZAID	Library	ZAID	Library
^{1}H	1001.60C	ENDF/B-VI	1001.42C	ENDL-92
^{10}B	5010.60C	ENDF/B-VI	5010.50C	RMCCS/B-V
^{11}B	5011.60C	ENDF/B-VI	5011.50C	ENDF/B-V
C	6000.60C	ENDF/B-VI	6000.50C	RMCCS/B-V
^{14}N	7014.60C	ENDF/T-2	7014.42C	ENDL-92
^{16}O	8016.60C	ENDF/B-VI	8016.42C	ENDL-92
^{19}F	9019.60C	ENDF/B-VI	9019.50C	ENDF/B-V
^{27}Al	13027.60C	ENDF/B-VI	13027.42C	ENDL-92
Si	14000.60C	ENDF/B-VI	14000.42C	ENDL-92
Fe	26000.55C	RMCCS/T-2	26000.42C	ENDL-92
Ni	29000.50C	RMCCS/B-V	29000.35C	ENDL-85
Cd	48000.51C	RMCCS/B-V	48000.42C	ENDL-92

The results for 144 keV, 1.2 and 5 MeV are given in Table 6. They show that using an older set of cross-sections has no noticeable effect on the values of efficiency and effective centre. However, it is possible that by changing all the cross sections at once, the effects have been at least partially cancelled out, i.e. applying the older cross sections for one isotope may increase the efficiency, but for another isotope the older cross sections may decrease the efficiency by a similar amount.

Table 6: Changes in the effective centre and efficiency of the NPL long counter when using older cross-section data

	144 keV			1.2 MeV			5.0 MeV		
Cross-sections	Default	Old	Change	Default	Old	Change	Default	Old	Change
Effective centre (cm)	-0.80 ± 0.13	-0.93 ± 0.11	-0.13	0.86 ± 0.19	0.52 ± 0.19	-0.34	3.38 ± 0.26	3.84 ± 0.27	+0.46
Efficiency (cm^2)	10.078 ± 0.093	10.144 ± 0.093	+0.066	11.215 ± 0.099	11.292 ± 0.098	+0.077	11.132 ± 0.097	11.191 ± 0.097	+0.059

2.3.5.5 Number of source to long counter distances

Instead of calculating the response at 50 distances from 115 to 600 cm, the number of distances was reduced to 25 by omitting alternate positions. Calculations for the NPL long counter were re-run with the number of histories for each run doubled to 10^6 to keep the total number of histories constant. The results are given in Table 7. For 144 keV, the change in the effective centre is slightly greater than the statistical uncertainty, but for 1.2 and 5 MeV the change is well within the uncertainty. This suggests that whether 50 or 25 distances are used makes no real difference to the result.

Table 7: Changes in the calculated effective centre of the NPL long counter with a change in the number of source to long counter distances

	144 keV			1.2 MeV			5.0 MeV		
No. of distances	50	25	Change	50	25	Change	50	25	Change
Effective centre (cm)	-0.80 ± 0.13	-1.30 ± 0.31	-0.50	0.86 ± 0.19	0.82 ± 0.10	-0.04	3.38 ± 0.26	3.29 ± 0.21	-0.09

2.3.5.6 Overall uncertainties

To simplify matters, single values for the effective centre and efficiency uncertainties will be applied for all energies and for both long counters.

The uncertainty in the effective centre values from the random number MCNP calculations is based on the standard error of the five runs. This gives uncertainties ranging from 0.04 to 0.39 cm. It is likely that most of the variation in the size of the uncertainty is because only 5 runs were performed. The sets of starting random numbers may not be sufficiently different to give a true spread of results with only five runs. The statistical component of the effective centre uncertainty was therefore taken as the maximum standard error for any energy (i.e. 0.39 cm).

The sensitivity analysis showed that the changes in the efficiency and effective centre due to small changes to the input data are generally within the statistically derived uncertainties. This is not to say that they have no effect but rather that the change in the result is hidden by the random uncertainty. To cover the uncertainty components studied in the sensitivity analysis, an estimated uncertainty of 0.50 cm, based on the largest observed change in the effective centre, was added in quadrature to give a combined effective centre uncertainty of 0.63 cm.

The MCNP parallel beam efficiency values of Tagziria[Ta98] have statistical uncertainties of 1% for both long counters. Based on the largest observed change in the efficiency from the sensitivity analysis, a further 1% was added in quadrature. This gives a combined uncertainty of 1.4%. The normalisation of calculations to measurements with radionuclide sources will also contribute to the overall uncertainty in the efficiency and this will be covered later in the report (Section 4).

2.4 Positions of interactions in the BF_3 tube

To examine the mechanisms that give rise to an energy dependent effective centre, the BF_3 tube in the De Pangher MCNP model was divided into 1 cm long segments along its length. The $^{10}B(n,\alpha)$ reactions were tallied in each segment and mean positions of the reactions were calculated for a number of incident neutron energies. The profiles are shown in Figure 12. As the neutron energy increases, the mean position of interactions moves along the tube, and the bulk of the interactions become spread over a greater range of the tube. The areas under the lines correspond to the overall efficiencies.

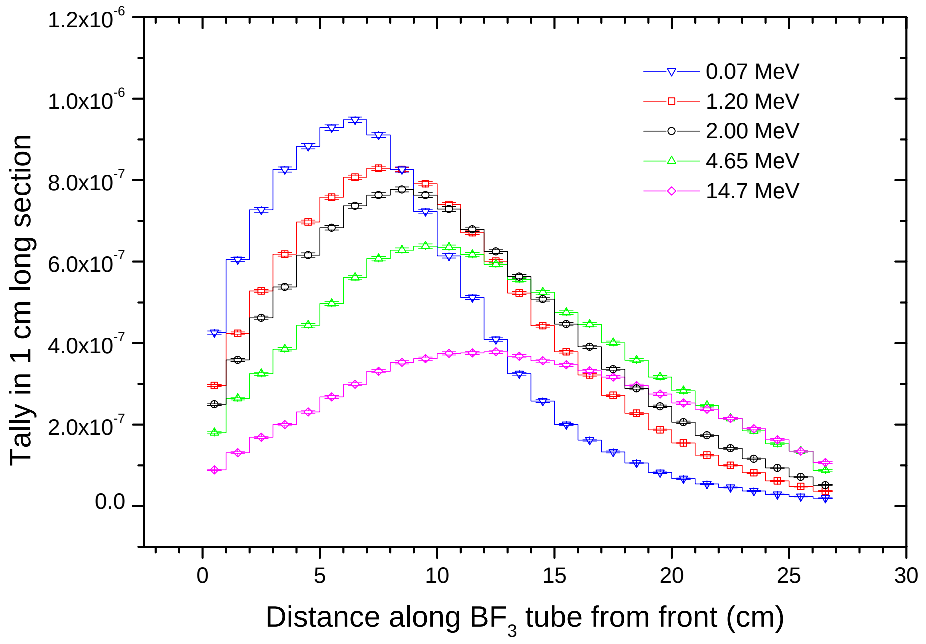

Figure 12: Profiles of $^{10}B(n, \alpha)$ interaction position in the BF_3 tube for different energies

A relationship was investigated between the mean interaction position and the calculated effective centre from the random number MCNP method by plotting them against each other. Figure 13 indicates that a linear relationship exists between the mean position of the BF_3 $^{10}B(n,\alpha)$ interactions and the effective centre. The front of the active part of the BF_3 tube corresponds to 0.0324 cm on the effective centre scale. The linear fit to the points indicates that a 1 cm change in the mean position of the BF_3 (n,α) interactions corresponds to a 1.1 cm change in the effective centre, with an offset of 7.7 cm. This supports the basic explanation that the position of the effective centre changes with energy because the distance the neutrons travel into the long counter before interacting in the BF_3 tube also has an energy dependence.

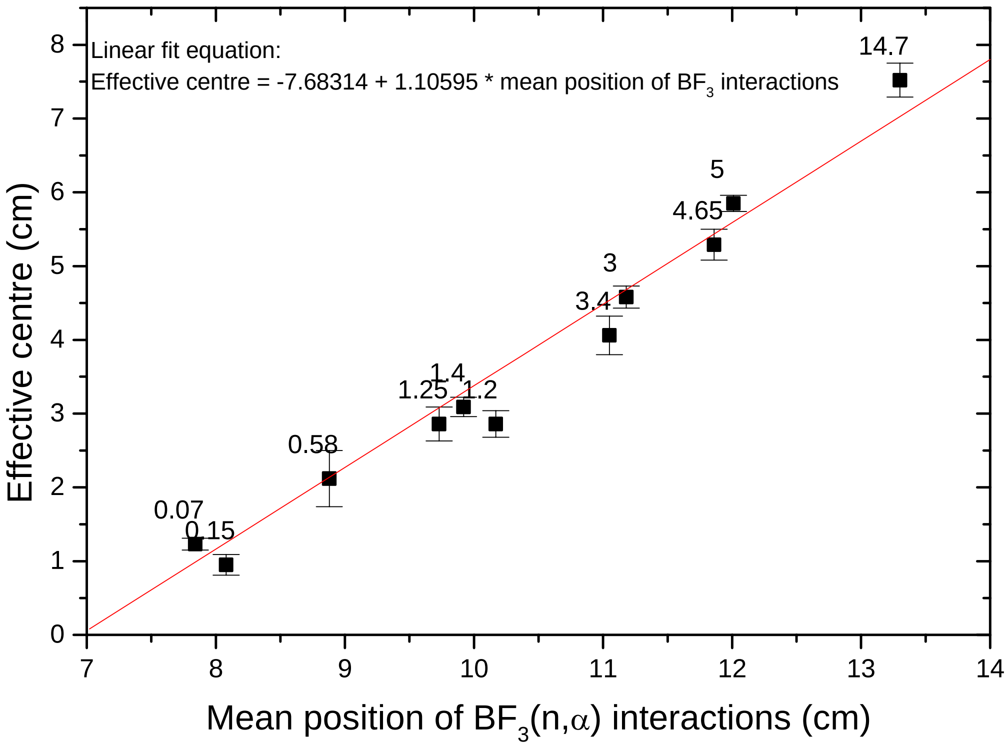

Figure 13: Effective centre versus mean position of BF_3 (n,α) interactions for the De Pangher long counter (points labelled with incident neutron energy in MeV)

2.5 Radial efficiency

To investigate how the efficiency of the De Pangher varies with radial distance from the central axis, the parallel beam model was adapted to irradiate the long counter with a ring of neutrons. The inner and outer radii of the rings coincided with cylindrical surfaces in the model (e.g. the edge of the BF_3 tube), and were sometimes broken down further in regions where cylindrical surfaces were far apart. Figure 14 shows the results for 144 keV, 565 keV, 1.2 MeV and 5.0 MeV. The efficiencies of each ring have been divided by the radial width so the shape is independent of the ring structure.

The relative shapes of the radial efficiency for the 3 energies are roughly as would be expected with the air ring in the front face of the moderator becoming more significant the lower the energy.

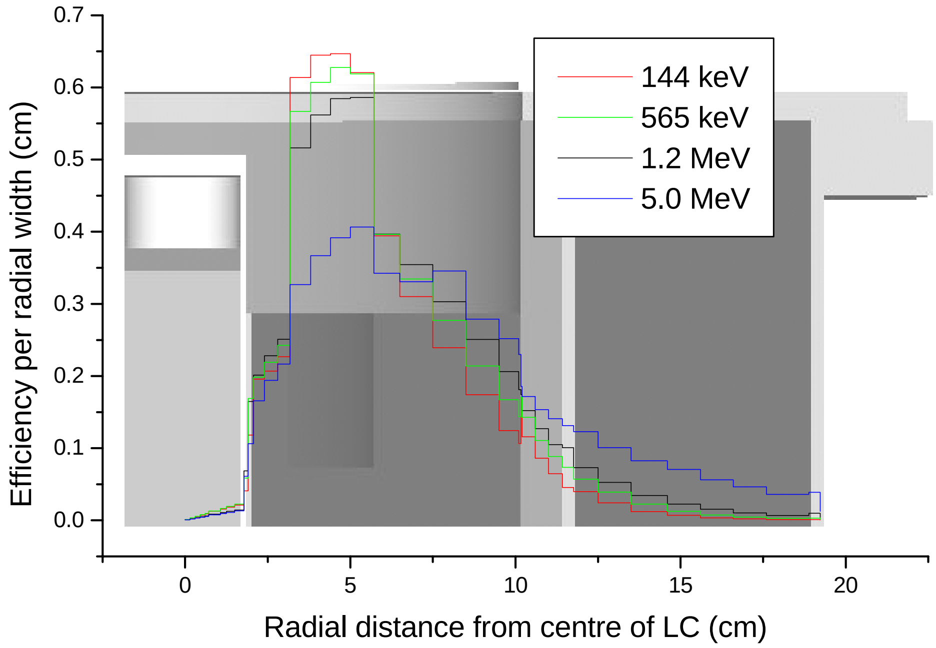

Figure 14: Radial efficiency of the De Pangher long counter for monoenergetic parallel beam neutrons. The front part of the MCNP geometry is superimposed for comparison

2.6 5″ Bonner Sphere

In order to validate the MCNP methods for calculating effective centres, the effective centre of a 5″ Bonner sphere model was determined with MCNP. For a spherical device the effective centre is conventionally taken as being at the centre of the sphere, although this assumption relies more on intuition than on calculations or measurements.

The MCNP model of the Bonner sphere was constructed by adding a 5 inch diameter polyethylene sphere to an existing model of an SP9-type He-3 counter (taken from the Tagziria model of the Harwell 0949 area survey instrument[Ba01]). The model was run with a point source with the ISO ^{241}Am-Be energy spectrum at exactly the same distances as the experiment described later in section 3.4, i.e. from 156.15 to 516.15 cm in 5, then 10, then 20 cm steps. Firstly, the source was biased using an exponential function with a = 3.5 as in the initial MCNP method used for long counter effective centres. This gave an effective centre of -0.1 ± 1.3 cm (a negative value indicating that it is in the direction of the source).

To more accurately simulate the experiment, the source was changed to a distributed source with the dimensions of an X14 capsule. The biasing was also changed to vary with distance to keep the sampling more uniform across the Bonner sphere while still improving the efficiency of the calculation. This gave an effective centre of (-0.05 ± 0.11) cm.

Both calculation methods gave answers which agreed with the expected result of 0 cm. This validates the methods and also the assumption that the effective centre of a spherical device is at the centre of the sphere. For the Bonner sphere there did not appear to be any of the random number correlation problems observed with the long counter calculations. This suggests that the complexity of the long counters, and the rapidly changing radial efficiency with radial distance, are the main causes of the effect.

3 MEASUREMENTS

Where calculated efficiencies are referred to in the following sections they have been normalised according to the factors outlined in section 4. The uncertainties in the calculated values are overall figures as described in section 2.3.5.6. The efficiency uncertainties also include a normalisation component (see sections 4.2 and 4.3).

3.1 De Pangher long counter

3.1.1 New measurements

In recent years a PC based data acquisition system has been developed at NPL using an MS-12 scaler card from FAST ComTec with in-house software written in Visual Basic 6.0. For the first time it has been possible to make automated effective centre measurements where the movement of the Pennine detector transport system[Pen] is integrated with the data acquisition system. The detector locations (i.e. where measurements are to be made) are programmed into the Pennine system with pause commands separating them. When the PC has finished its preset number of cycles at a particular position it sends a signal to the Pennine instructing it to continue with the program. When the detector has reached the new position a signal is sent back from the Pennine system to the PC and the acquisition of data starts again. A relay unit was required to interface between the TTL voltages of the PC and the 24 V architecture of the Pennine system.

As the erection of shadow cones has to be performed manually, effective centre measurements usually break down into 4 or 6 components - 2 or 3 shadow cones are required to cover the full range of distances, and for each range “total” (i.e. without shadow cone) and “scatter” (i.e. with shadow cone) measurements are required. Once set-up, a radionuclide source measurement can be left to run overnight or over a weekend to make full use of time in the NPL low scatter facility. The output data are in the form of a text file with clear labelling of the positions of the detector.

3.1.1.1 ^{252}Cf

The automated system was used to measure the effective centre and efficiency of the De Pangher long counter with a ^{252}Cf source (serial number 4774NC, approx. 5 μg, in a modified X35 capsule). Measurements were made at 49 distances from 150 to 500 cm, with changes of shadow cone at 250 and 420 cm. The effective centre was determined to be (2.60 ± 0.15) cm, and the efficiency (3.313 ± 0.024) cm^2.

In calculating the emission rate of the source on the days of the measurement, a fit to the manganese bath measurements performed over the years was used which allowed for the presence of the ^{250}Cf isotope. The emission rate measurements were based on new, MCNP calculated, correction factors for neutron losses in the bath[Ro01], and these give results which are approximately 0.75% higher than those obtained using the older correction factors. The value of the efficiency would therefore be expected to be lower than previously measured. This is the case although the decrease is 4.5% when compared to the measurement of Hunt (3.47 ± 0.03 cm^2)[Hu76] and 2.3% when compared to the measurement of Tagziria (3.39 ± 0.02 cm^2)[Ta98].

Agreement with the MCNP parallel beam calculated efficiency value of (3.400 ± 0.054) cm^2 is just outside of the 1 sigma uncertainties, as is the random number MCNP calculated effective centre of (3.51 ± 0.63) cm.

In order to compare the different values of effective centre and efficiency, the source emission rate was calculated from the measurement at each distance using efficiency and effective centre values derived from: the experimental values of this work, the measurements of Tagziria, Hunt, and also the calculated values from the two MCNP methods. These are shown in Figure 15 together with the fitted value of emission rate from manganese bath measurements. The uncertainties shown in the graph correspond to the components that are uncorrelated for the measurement at each source to long counter distance, i.e. the uncertainties in the efficiency and effective centre, not the uncertainties in the individual long counter count rate measurements. In the absence of covariance values for the previous efficiency and effective centre values, for the purposes of this comparison they have been treated as uncorrelated.

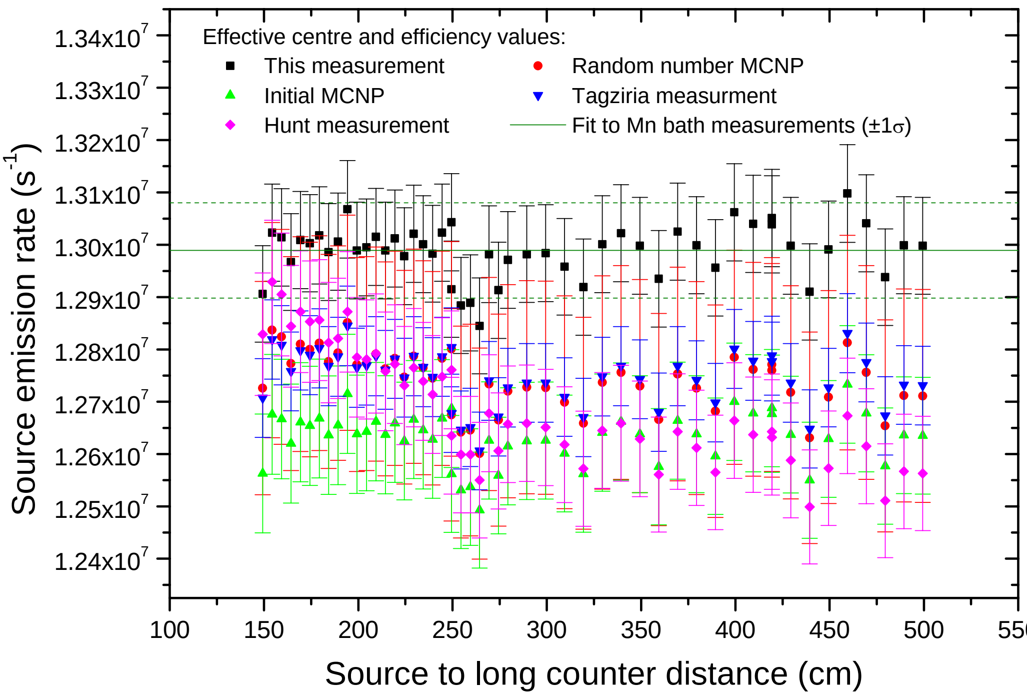

Figure 15: Comparison of ^{252}Cf source emission rates from De Pangher long counter measurements analysed using different effective centre and efficiency values

The graph shows that at a typical measurement position of 2 m, the source emission rate, and therefore the fluence, would be underestimated by 1.6% using the parameters from the Hunt measurement, by 1.7% using the parameters from the Tagziria measurement, or by 1.7% using the new MCNP calculated parameters. As explained above, some of the difference between old and new measurements will be due to changes in the manganese bath correction factors and impurity levels over the last 30 years, and for the Tagziria measurement allowance may not have been made for the ^{250}Cf content of the source. However the Hunt values produce a downward trend with distance, which suggests that the effective centre value is too large. The discontinuity at 250 cm coincides with the change of shadow cone, and suggests that from 250 to 270 cm the cone is not adequately shielding the long counter from direct neutrons.

3.1.1.2 ^{241}Am-Li

Using the automated system, the effective centre and efficiency of the De Pangher long counter was measured with a ^{241}Am-Li source (serial number AMN5000/3250Li, 185 GBq (5 Ci) in an X14 capsule). Measurements were made at 51 distances from 150 to 500 cm, with a change of shadow cone position occurring at 300 cm. The effective centre was determined to be (3.5 ± 1.2) cm, and the efficiency (3.460 ± 0.042) cm^2.

Within the rather large uncertainties, this value of effective centre agrees with the measurement of Hunt[Hu76] of (1.52 ± 1.78) cm, and with the random number MCNP value of (1.70 ± 0.63) cm. The value of efficiency presented here also agrees with Hunt's measurement of (3.36 ± 0.06) cm^2 and with the parallel beam MCNP value of (3.400 ± 0.054) cm^2.

To compare the different values of effective centre and efficiency, the source emission rate was calculated from the measurement at each distance using efficiency and effective centre values derived from: the experimental values of this work, the measurement of Hunt, and also the calculated values from the random number MCNP method. These are shown in Figure 16 together with the decay corrected value of the emission rate from a manganese bath measurement. The uncertainties shown in the graph correspond to the components that are uncorrelated for each source to long counter distance, as described earlier in section 3.1.1.1.

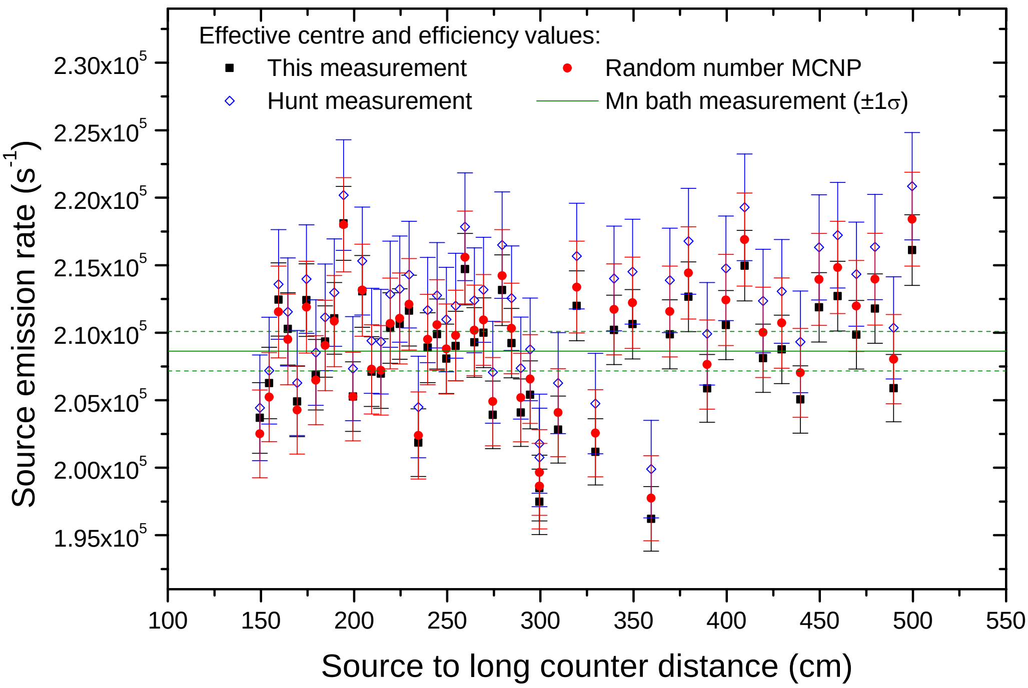

Figure 16: Comparison of ^{241}Am-Li source emission rates from De Pangher long counter measurements analysed using different effective centre and efficiency values

The graph shows that when values of efficiency and effective centre from the same measurement or calculation method are used together, the derived source emission rates, and hence fluences, are not significantly different. At distances of 150-250 cm, where fluence measurements are typically made, the agreement with the manganese bath source emission rate is very good when applying the random number MCNP efficiency and effective centre.

3.1.1.3 1.2 MeV

In 2001 measurements were made[Th01] using the Van de Graaff accelerator to produce 1.2 MeV neutrons. Total and scatter rates were measured at 21 distances from 150 to 500 cm. The effective centre was determined to be (1.68 ± 0.78) cm, which agrees within the uncertainties with the random number MCNP method result of (2.86 ± 0.63) cm. The new measured value is much closer to the calculated value than the measurements of either Hunt (4.50 ± 0.53 cm)[Hu76] or Tagziria (-0.16 ± 0.41 cm)[Ta98].

3.1.1.4 5 MeV

Using quasi-monoenergetic 5 MeV neutrons from the Van de Graaff accelerator, measurements were made in 2001[Th01] at 35 distances from 150 to 490 cm. The effective centre was determined to be (5.49 ± 0.87) cm. This agrees very well with the random number MCNP method result of (5.85 ± 0.63) cm.

3.1.2 Review of previous measurements

Although all De Pangher long counters are made to the same design, comparing measurements made by different laboratories on different counters is not straightforward. Different methods of analysis and measurement techniques are used by various authors (discussed in [Hu72]), some assume constant in-scatter and only make measurements close to the source, and there may also be manufacturing differences between similar long counters. For those reasons Table 8 only includes measurements made with the De Pangher long counter of NPL in the low scatter facility at NPL.

Table 8: Effective centre measurements with radionuclide sources made using the NPL De Pangher long counter

Work	^{252}Cf	^{241}Am-Be	^{241}Am-Li	^{241}Am-B	^{241}Am-F	^{238}Pu-Li	^{226}Ra-Be	^{124}Sb-Be
[Ta98]	3.17 ± 0.10	4.59 ± 0.26			4.07 ± 0.99	3.49 ± 0.50		
[Hu76]	6.27 ± 0.61	8.12 ± 0.46	1.52 ± 1.78	6.73 ± 0.78*			2.39 ± 2.16	2.70 ± 1.70
[Mo89]	3.76 ± 0.28							
[Ta01]								0.21 ± 0.52 -0.82 ± 0.61
Roberts04	2.60 ± 0.15		3.5 ± 1.2					

* unpublished measurement by Hunt

Table 9: Effective centre measurements with monoenergetic neutrons made using the NPL De Pangher long counter

Work	144 keV	565 keV	1.2 MeV	2.5 MeV	5 MeV
[Ta98]	-1.09 ± 0.52	1.88± 0.24	-0.16 ± 0.41	3.52 ± 0.40	8.28 ± 0.75
[Hu76]		3.00± 0.52	4.50± 0.53	7.09 ± 0.58	
[Th01]			1.68 ± 0.78		5.49 ± 0.87

Over the years, the effective centres of other De Pangher long counters have been measured at NPL and elsewhere. Table 10 summarises these values.

Table 10: Effective centre measurements made using other De Pangher long counters

Work	^{252}Cf	^{241}Am-Be	^{241}Am-Li	^{226}Ra-Be	^{124}Sb-Be	2.7 MeV
[Th03]						3.05 ± 0.70
[Th91]	3.80 ± 1.00	9.90 ± 1.00				
[Hu89]	4.20 ± 1.00	5.13 ± 1.76				
[Ta97]	3.00 ± 1.20	4.60 ± 1.60				
[Th72]		7.74 ± 0.31		2.10 ± 2.04	-0.14 ± 1.02	
[Ma72]	3.78 ± 0.20	6.17 ± 0.38				
[De66]		5.25 ± 0.20		1.65 ± 0.10	1.65 ± 0.30	
[Mi72]	3.85 ± 0.30	5.85 ± 0.40	2.45 ± 0.20		1.35 ± 0.20	
[He73]	4.70 5.80	5.30 6.30	3.70 4.80	3.20 4.00	2.60 4.00	

All De Pangher long counter effective centre measurements are plotted in Figure 17, with the range up to 2.5 MeV shown in more detail in Figure 18. It can be seen that the measurements and fit made by Hunt do not agree with the random number MCNP calculations nor with a large number of other measurements. The monoenergetic measurements of Tagziria[Ta98] generally disagree with the MCNP calculations, whereas the same measurements made by Thomas and Roberts[Th01] show much better agreement. An explanation for this may be that the measurements of Tagziria were made using higher beam currents on the targets. This can lead to heating of the target and a change in the target characteristics. As measurements are normalised to the current on the target, any changes in the yield or energy of the neutrons will go unnoticed and so the equations given in section 2.2 could not be correctly applied for measurements made at different distances.

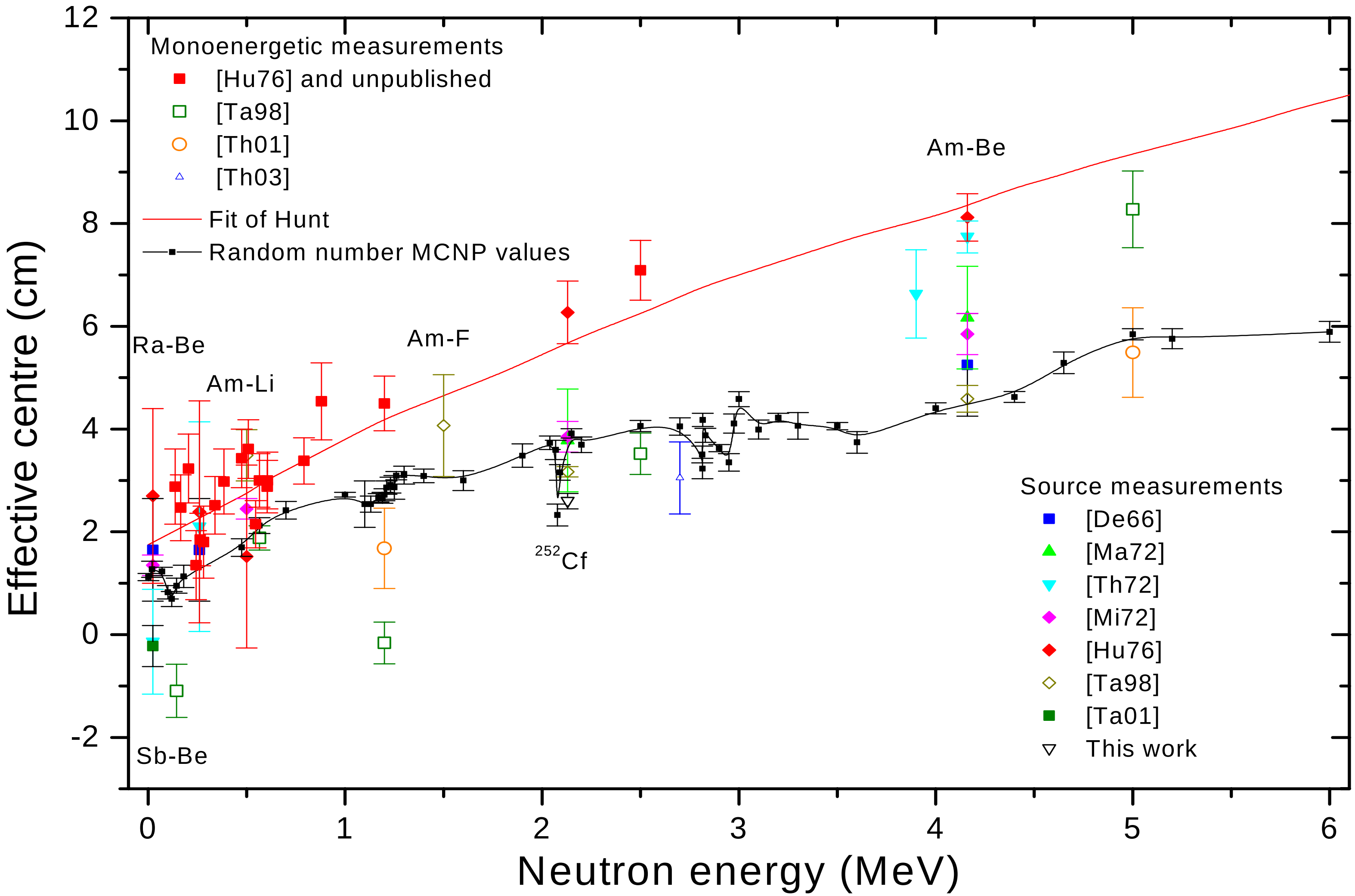

Figure 17: Effective centre measurements for a De Pangher long counter and comparison with the fit of Hunt[Hu76] and the new MCNP calculations (MCNP error bars represent statistical component only)

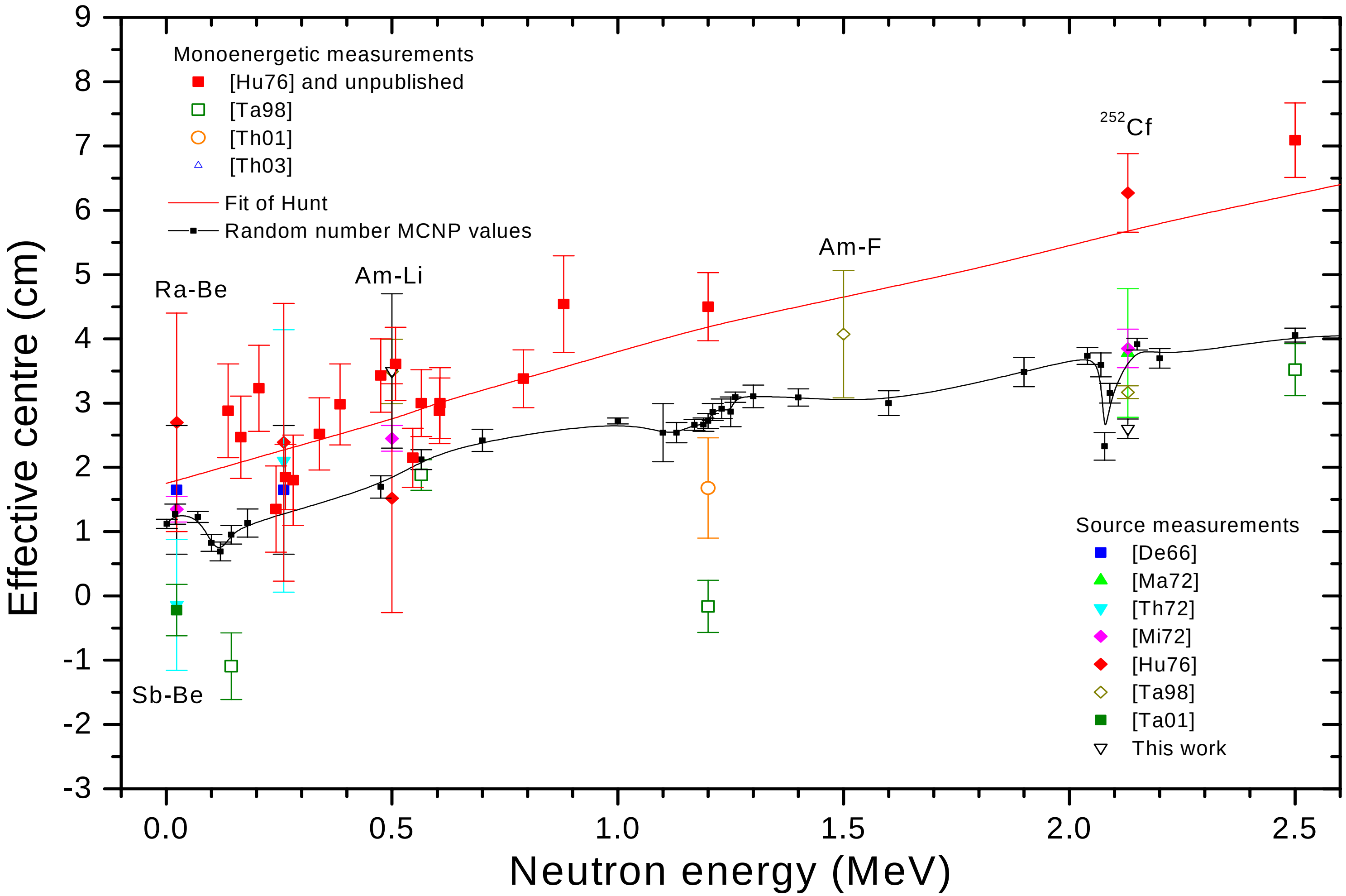

Figure 18: Effective centre measurements up to 2.5 MeV for a De Pangher long counter and comparison with the fit of Hunt[Hu76] and the new MCNP calculations (MCNP error bars represent statistical component only)

3.2 NPL long counter

3.2.1 New measurements

The automated data acquisition and Pennine control system described in section 3.1.1 was also used to make effective centre measurements of the NPL long counter for radionuclide sources. Parallel beam MCNP calculated efficiencies used in this section to compare with measurements have been normalised as described later in Section 4.3.

3.2.1.1 ^{252}Cf

A ^{252}Cf source (serial number 4774NC, approx. 5 μg, in a modified X35 capsule) was used for the measurement. Measurements were made at 49 distances from 150 to 497 cm, with changes of shadow cone occurring at 250 and 420 cm. The effective centre was determined to be (1.91 ± 0.20) cm, and the efficiency (12.27 ± 0.11) cm^2.

This measured effective centre value is 0.58 cm greater than the MCNP random number calculated value of (1.33 ± 0.63) cm, and therefore agrees within the uncertainties. However the agreement with calculation is much better than with the Hunt measured value of (3.486 ± 0.276) cm.

The emission rate of the source was determined using the method described in section 3.1.1.1 to allow for the presence of the ^{250}Cf isotope. The new efficiency is 3.6% lower than the measurement of Hunt (12.73 ± 0.08 cm^2) and 1.9% lower than the measurement of Tagziria (12.51 ± 0.07 cm^2). There is good agreement with the normalised parallel beam MCNP calculated value of (12.49 ± 0.21) cm^2.

3.2.1.2 ^{241}Am-Be

A 37 GBq (1 Ci) ^{241}Am-Be source in an X3 capsule (serial number AMN1000/1095) was used for the measurement. Measurements were made at 49 distances from 150 to 497 cm, with a change of shadow cone occurring at 280 cm. The effective centre was determined to be (3.96 ± 0.24) cm, and the efficiency (12.102 ± 0.088) cm^2. The effective centre is over 1.5 cm greater than the random number MCNP method value of (2.27 ± 0.63) cm, but agrees with the measurement of Tagziria given in Table 11. The Hunt measurement given in the table is considerably greater than recent measurements.

The value of efficiency from this measurement agrees very well with the Tagziria measured value of (12.121 ± 0.075) cm^2 and also the Hunt measured value of (12.15 ± 0.10) cm^2. In addition, there is agreement with the normalised parallel beam MCNP calculated efficiency of (12.31 ± 0.21) cm^2.

3.2.1.3 ^{241}Am-Li

A 185 GBq (5 Ci) ^{241}Am-Li source in an X14 capsule (serial number AMN5000/3250Li) was used for the measurement. Measurements were made at 51 distances from 150 to 497 cm, with a change of shadow cone position occurring at 300 cm. The effective centre was determined to be (1.07 ± 0.69) cm, and the efficiency (12.34 ± 0.11) cm^2. The effective centre is in agreement with Hunt's measured value given in Table 11, and also with the random number MCNP method value of (-0.05 ± 0.63) cm.

The value of efficiency measured here agrees with the measured value of Hunt of (12.27 ± 0.14) cm^2, and is almost in agreement with the normalised MCNP parallel beam calculation, which gives an efficiency of (11.99 ± 0.20) cm^2. The calculated efficiency is 2.8% lower than the measured value.

Using the normalisation factor of [Ta98] gives a calculated value that is 4.1% lower than the measured value, which is remarkably similar to the difference of 4.2% between measured and calculated efficiency for the ^{238}Pu-Li source in [Ta98]. The ^{124}Sb-Be normalised efficiency calculation was lower than the measurement by 4.9% in [Ta01]. The ^{241}Am-Li and ^{238}Pu-Li sources are believed to have very similar energy spectra with mean energies of around 0.5 MeV, whilst the ^{124}Sb-Be photo-neutron source emits neutrons with energies of about 23 keV. This suggests that there is a problem with either calculation or measurement at low neutron energies.

However, the De Pangher long counter efficiency measurements and calculations for the ^{238}Pu-Li and ^{124}Sb-Be sources do not show a similar disagreement. This would rule out a problem with the measurement technique, for instance the scatter correction, and so the more likely cause is the model. This is discussed further in the section on normalisation (4.3).

To test if normalising the calculations by increasing the BF_3 pressure in the model would have a greater effect on lower energy neutron spectra, the parallel beam model was run for both ^{241}Am-Be and ^{241}Am-Li with the BF_3 atomic density increased by 10 and 21%. There was no noticeable difference in the increase in efficiency between the two energy spectra. For 10 and 21% increases in the density, the efficiency increased by 5.76 and 11.74% respectively.

Figure 19 shows the effect of using the different values for effective centre and efficiency when calculating the emission rate of the Am-Li source from the measurements made at each distance. The uncertainties in the graph are the uncorrelated components only, as described in section 3.1.1.1. None of the three effective centre values produces a noticeable trend with distance, suggesting that they are all approximately correct. However the MCNP calculated efficiency and effective centre leads to an overestimation of the emission rate, and hence the fluence, of 2.0% averaged over all distances.

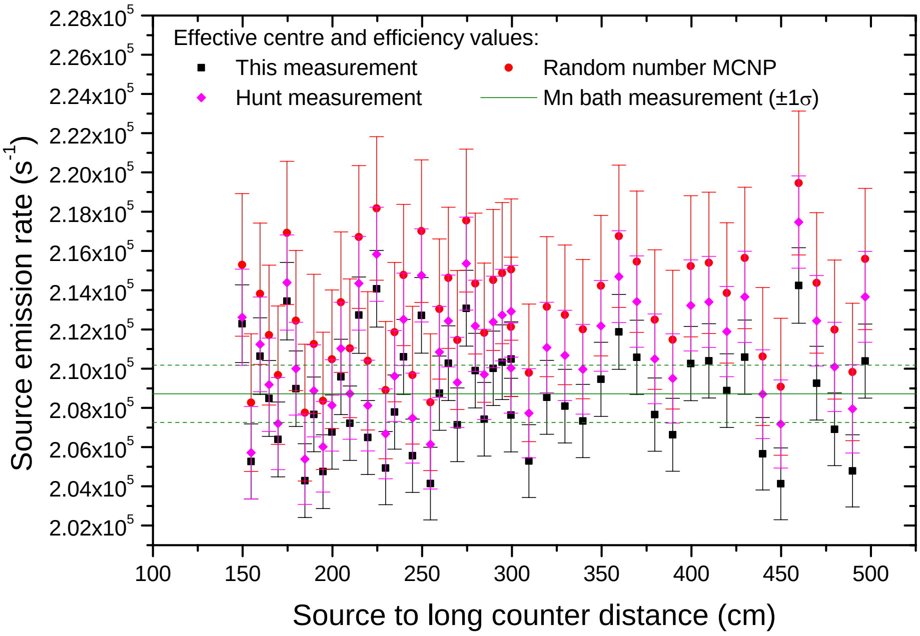

Figure 19: Comparison of ^{241}Am-Li source emission rates from NPL long counter measurements analysed using different effective centre and efficiency values

3.2.1.4 565 keV

Using 565 keV neutrons from the Van de Graaff accelerator, measurements were made at only 9 distances from 150 to 495 cm. The effective centre was determined to be (-0.15 ± 0.42) cm. This agrees with the random number MCNP method result of (-0.54 ± 0.63) cm.

3.2.1.5 1.2 MeV

Monoenergetic 1.2 MeV measurements were made at 35 distances from 140 to 460 cm. The effective centre was determined to be (0.54 ± 0.22) cm. This agrees with the random number MCNP method result of (0.86 ± 0.63) cm, but strongly disagrees with the values of Hunt and Tagziria given in Table 11.

3.2.2 Review of previous measurements

As the NPL standard long counter is the only one of its exact type, the only comparison that can be made is with previous measurements of the same instrument which have always been carried out in the NPL low scatter facility. The values are summarised in Table 11.

Table 11: Effective centre measurements made using the NPL long counter

a) Radionuclide sources

Work	^{252}Cf	^{241}Am-Be	^{241}Am-Li	^{241}Am-B	^{241}Am-F	^{238}Pu-Li	^{226}Ra-Be	^{124}Sb-Be
[Ta98]	0.90 ± 0.12	3.57 ± 0.28		2.66± 0.32	0.50 ± 0.67	3.6 ± 1.3		
[Hu76]	3.46 ± 0.27	6.22 ± 0.53	-0.42 ± 1.04	3.89 ± 1.18*		-0.85 ± 0.66†	1.7 ± 1.0**	-0.72 ± 0.44‡
[Ta99]	1.70 ± 0.28							
[Ta01]								-1.25 ± 0.42 -1.26 ± 0.47
Roberts04	1.91± 0.20	3.96 ± 0.24	1.07 ± 0.69					

* Unpublished measurement made in 1982 using 13 points.
† Unpublished measurement made in 1986 using 21 points.
** Unpublished measurement made in 1973 using 31 points.
‡ Unpublished measurement made in 1978.

b) Monoenergetic fields

Work	144 keV	565 keV	1.2 MeV	2.5 MeV	5 MeV
[Ta98]	-1.76 ± 0.23	1.45 ± 0.29	4.12 ± 0.48	4.91 ± 0.25	8.33 ± 0.35
[Hu76]		0.89 ± 0.33	3.34 ± 0.43	5.59 ± 0.54	
[Th00][Th03]		-0.15 ± 0.42	0.54 ± 0.22		

Figure 20 plots the measurements alongside the fit of Hunt and the new MCNP calculated values, with the range up to 2.5 MeV shown in more detail in Figure 21. As for the De Pangher long counter, the measurements and fit of Hunt disagree with the MCNP calculations and most of the recent measurements particularly at high energies. The Tagziria monoenergetic measurements agree much better with the fit of Hunt than with the MCNP calculations. However the repeat measurements of Thomas at 565 keV and 1.2 MeV agree very well with the MCNP values. The use of higher beam currents, as mentioned in section 3.1.2, could provide an explanation of why the Tagziria values disagree by so much.

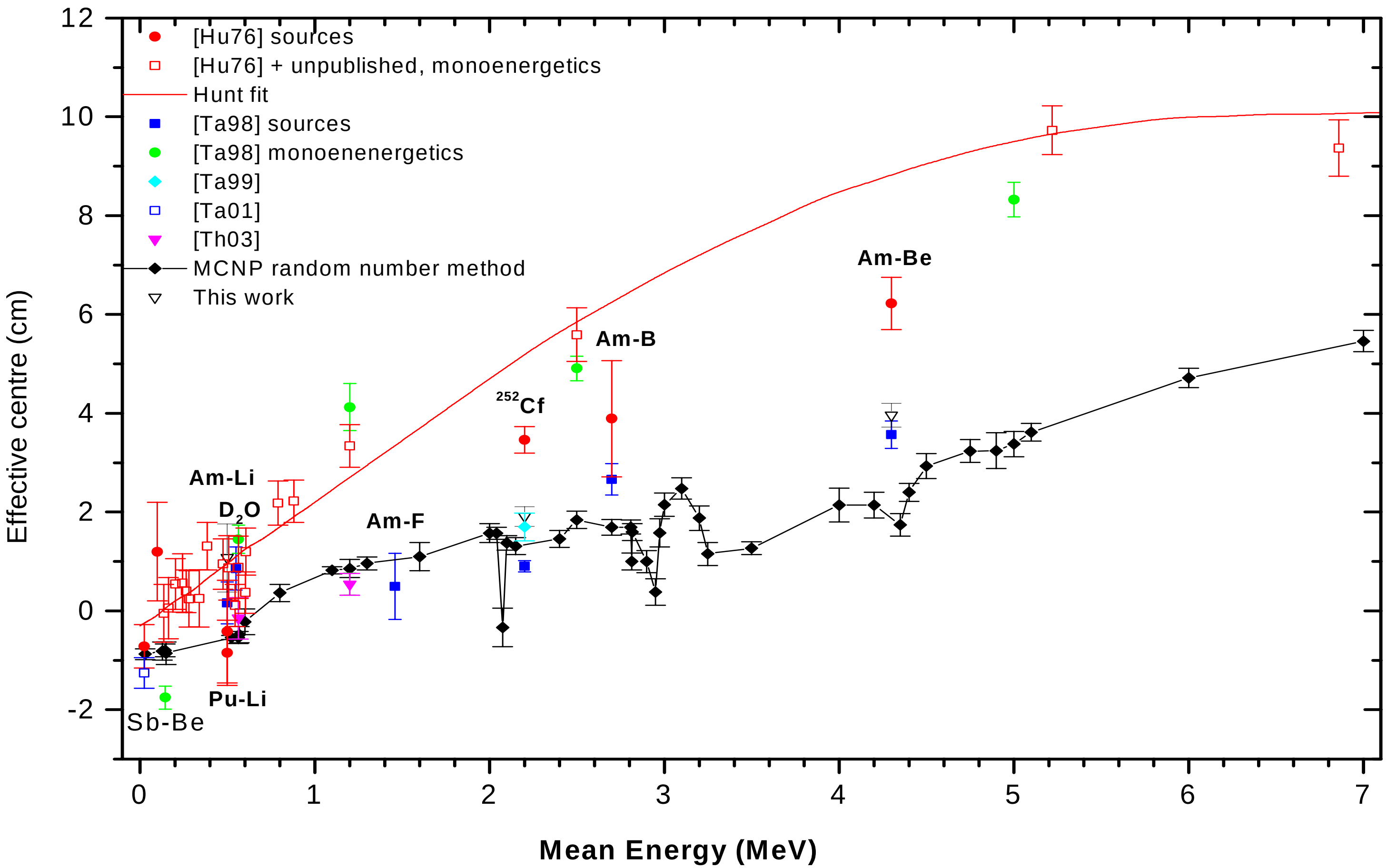

Figure 20: Effective centre measurements for the NPL long counter and comparison with the fit of Hunt and the new MCNP calculations (MCNP error bars represent statistical component only)

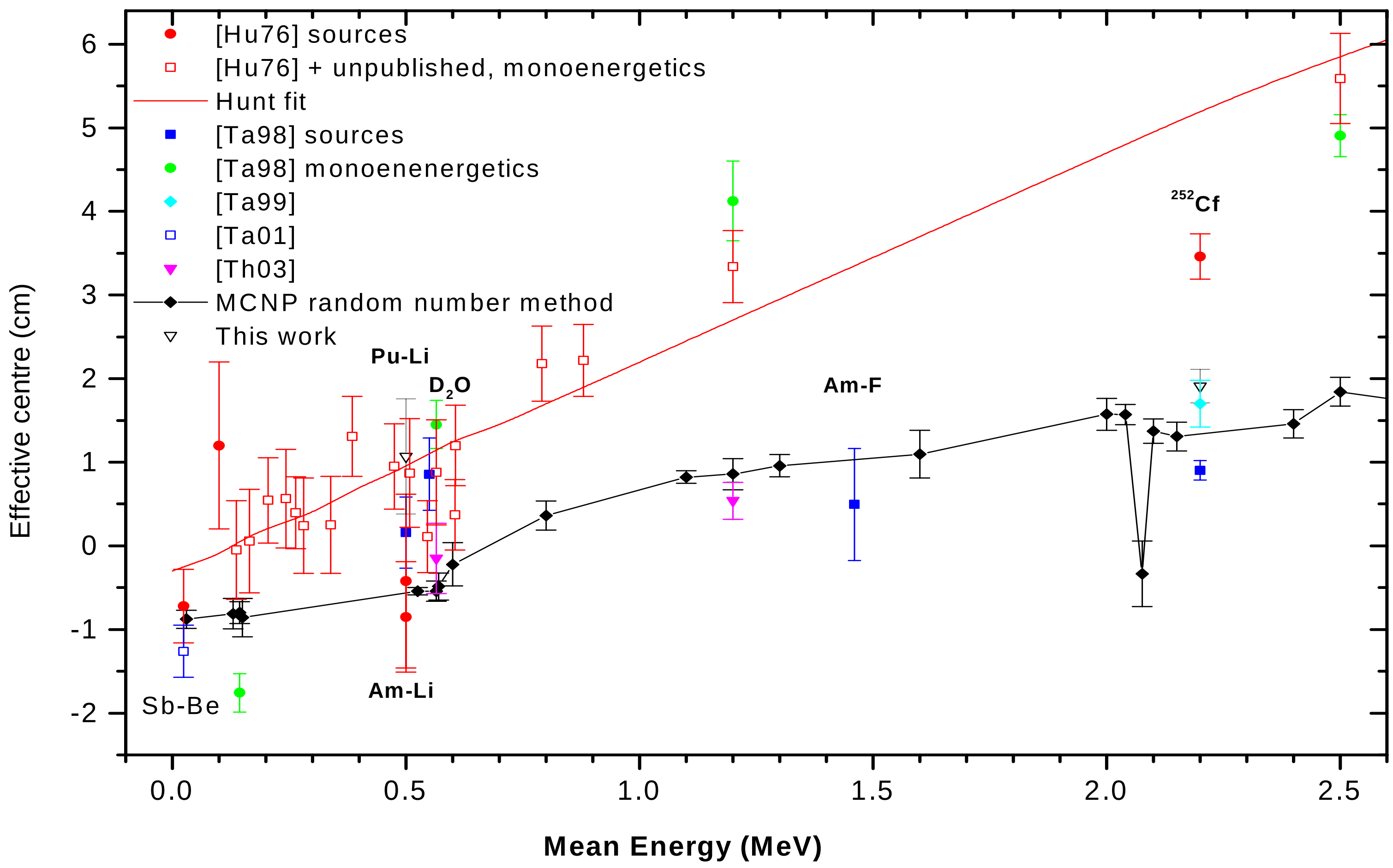

Figure 21: Effective centre measurements up to 2.5 MeV for the NPL long counter and comparison with the fit of Hunt and the new MCNP calculations (MCNP error bars represent statistical component only)

3.3 PTB intercomparison results

In March 2001, a Comité Consultatif pour les Rayonnements Ionisants (CCRI) intercomparison of the measurement of monoenergetic neutron fluence was held at the Physikalisch-Technische Bundesanstalt (PTB), Braunschweig, Germany. NPL participated using the De Pangher long counter for 144 keV, 1.2 MeV, 5 MeV, and 14.8 MeV. Fluence measurements were made at a number of distances, providing an opportunity to compare results using values of effective centre and efficiency from the initial and random number MCNP methods, and the fit of Hunt. The fluence normalised to a monitor and corrected to a distance of 1 m should be the same for all measurements at the same energy. The exercise also enabled measurements made with the De Pangher to be compared with measurements made by other laboratories using alternative methods to determine the fluence. An instrument referred to as the “New Monitor” was used to normalise the measurements.

For each nominally monoenergetic field, the true energy spectrum, calculated by the TARGET code[Sc98], was supplied by PTB. This enabled the effective centres calculated from MCNP based methods to be derived for the specific spectra rather than for just pure monoenergetic sources. Using the initial MCNP method, the TARGET spectra were entered directly into the MCNP input file. This yielded some unrealistic answers as highlighted in the plot of effective centre against energy near 1.2 MeV (Figure 22). The value found using the TARGET spectrum is much greater than any of the monoenergetic points within the energy range of the spectrum. There is no explanation for how this could be the case for the actual long counter and so it must be due to problems with the model and the method used to derive effective centres as described in section 2.3.1. Because of this problem, the effective centre values used by NPL in the CCRI exercise were obtained by taking the mean of monoenergetic values from the initial MCNP method weighted according to the TARGET spectra.

The random number MCNP method does not suffer from the same degree of inconsistencies when calculating values from spectra. Values of effective centre were therefore calculated by using the TARGET spectra directly in the MCNP input file. The TARGET code allows for scattering in the target, and the spectrum used for the MCNP calculation for 1.2 MeV thus included lower energy neutrons, roughly 3% in total, in the region below 1.2 MeV where the effective centre value is smaller. This is a likely explanation for the fact that the calculated effective centre for the spectrum is slightly lower than the point data around 1.2 MeV. However, the value is far more consistent with the monoenergetic values over the range of the TARGET energy spectrum than that obtained with the initial method, and so the random number MCNP method effective centre values presented in this section come from using the TARGET spectrum directly in MCNP using 50 distances.

For the initial MCNP based calculation method, the values for the efficiency came from averaging the monoenergetic values of Tagziria[Ta98] which were weighted according to the TARGET spectra. The efficiencies used with the random number MCNP method effective centres were calculated using the MCNP parallel beam model with the increased BF_3 density, described in section 2.3.3.

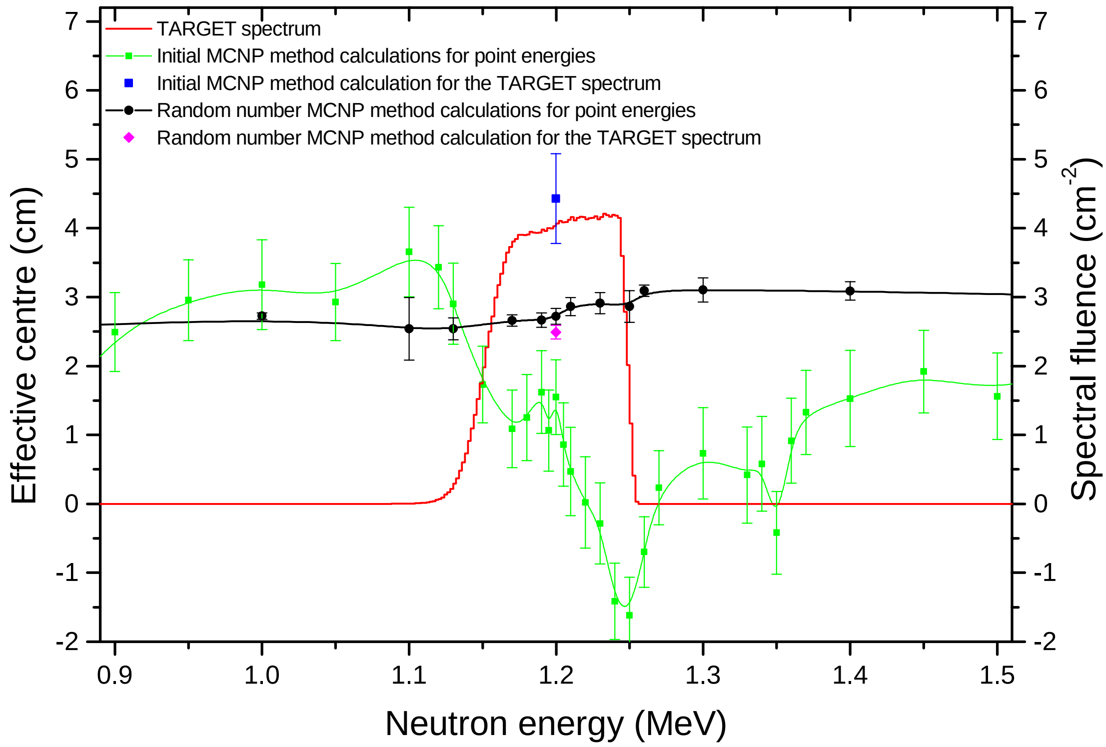

Figure 22: Comparison of 1.2 MeV De Pangher effective centres using the initial and random number MCNP methods (line connecting MCNP points intended as a guide only). The 1.2 MeV TARGET spectrum is also shown.

3.3.1 144 keV

The efficiency and effective centre values derived from the two calculational approaches and the fit of Hunt are shown in Table 12. At this energy, the random number MCNP method gives fluence values which agree better with the weighted mean from all participants in the intercomparison than the initial MCNP method (see Figure 23). However the Hunt fit agrees best of all with the weighted mean. It should be noted that the error bars for fluence measurements at a particular distance plotted in Figure 23 and subsequent figures correspond to estimates of the uncertainties which are **not** common to measurements at different distances, i.e. the uncorrelated components. The uncertainties which are effectively 100% correlated, e.g., the De Pangher efficiency, were excluded. The components which were included in the error bars were those due to: statistics, uncertainty in the dead time correction (taken to be 10% of the correction), and a component for the uncertainty in the distance *r*. The total uncertainty from all sources is ±2.2% at 1 sigma, which is sufficient to include the mean of all participants within the error bars for the fluence determined using the random number MCNP method effective centre.

Table 12: Effective centre and efficiency values for the De Pangher long counter at 144 keV

Method	Effective centre (cm)	Efficiency (cm^2)
Hunt fit	2.04	3.280
Initial MCNP	2.08	3.194
Random number MCNP	0.74	3.202

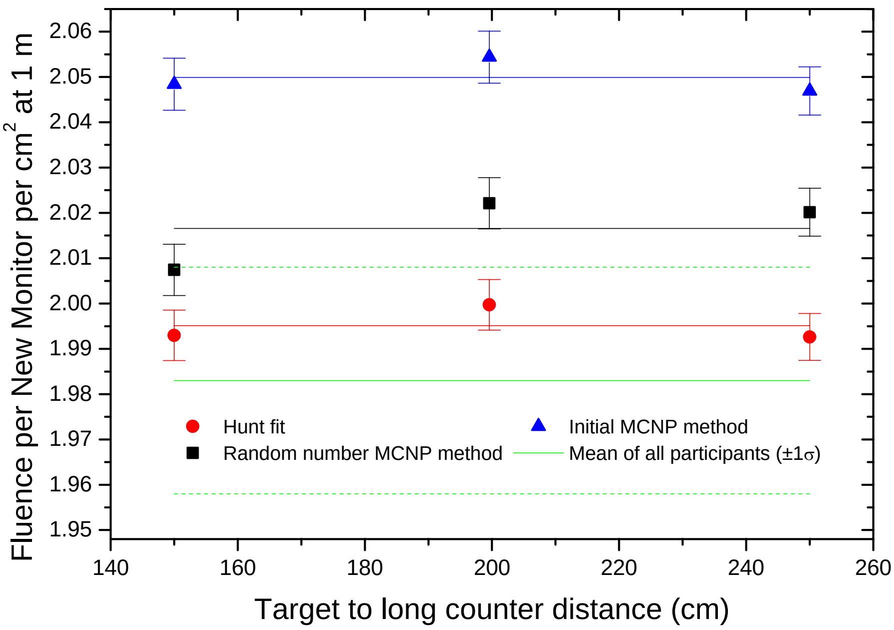

Figure 23: De Pangher 144 keV fluence results using efficiencies and effective centres from Hunt's fit, the initial MCNP method and the random number MCNP method (solid lines represent mean values)

3.3.2 1.2 MeV

Table 13 shows the efficiency and effective centre values derived from the two calculational approaches and the fit of Hunt. The graph of measured fluence versus distance (Figure 24) shows that the random number method gives the best results both in terms of agreement with the mean of all participants, and in terms of the effective centre. To see the latter, note that there is no trend in the derived fluence at 1 m with the target to long counter distance which indicates that the correct effective centre has been applied. The trend of points calculated using the fit of Hunt suggests that the value of effective centre is too far into the long counter, causing the near-in points to be too high. The opposite is true for the initial MCNP method effective centre value.

Table 13: Effective centre and efficiency values for the De Pangher long counter at 1.2 MeV

Method	Effective centre (cm)	Efficiency (cm^2)
Hunt fit	4.20	3.685
Initial MCNP	0.54	3.460
Random number MCNP	2.49	3.451

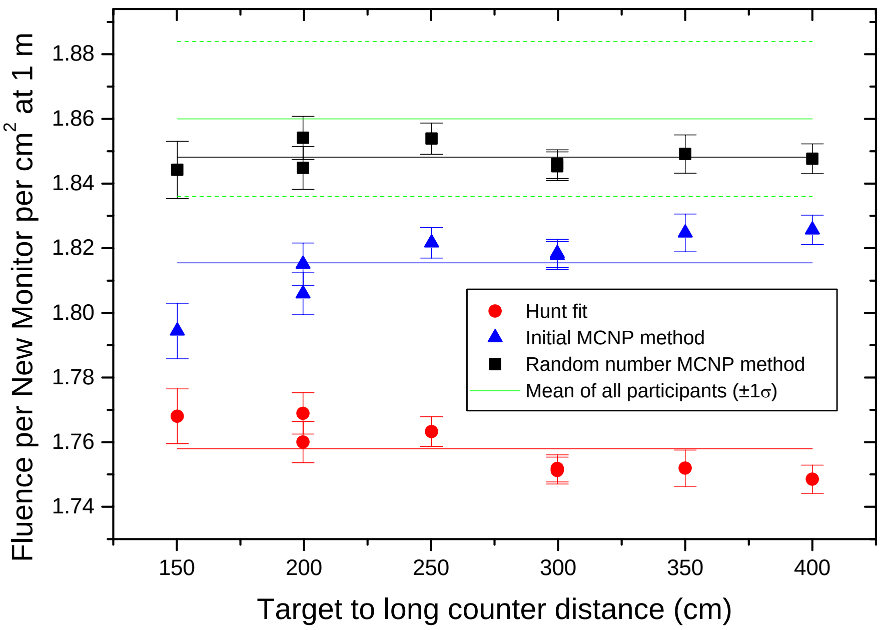

Figure 24: De Pangher 1.2 MeV fluence results using efficiencies and effective centres from Hunt's fit, the initial MCNP method and the random number MCNP method (solid lines represent mean values)

3.3.3 5.0 MeV

The efficiency and effective centre values derived from the two calculational approaches and the fit of Hunt are shown in Table 14. The graph below (Figure 25) shows that none of the three methods for determining the effective centre gives a particularly satisfactory result for 5.0 MeV. The upward trend indicates that the true effective centre is further into the long counter than all three methods suggest. However the mean fluence from each of the methods is within one standard deviation of the mean of all participants.

Table 14: Effective centre and efficiency values for the De Pangher long counter at 5.0 MeV

Method	Effective centre (cm)	Efficiency (cm^2)
Hunt fit	9.29	3.408
Initial MCNP	6.87	3.334
Random number MCNP	5.22	3.367

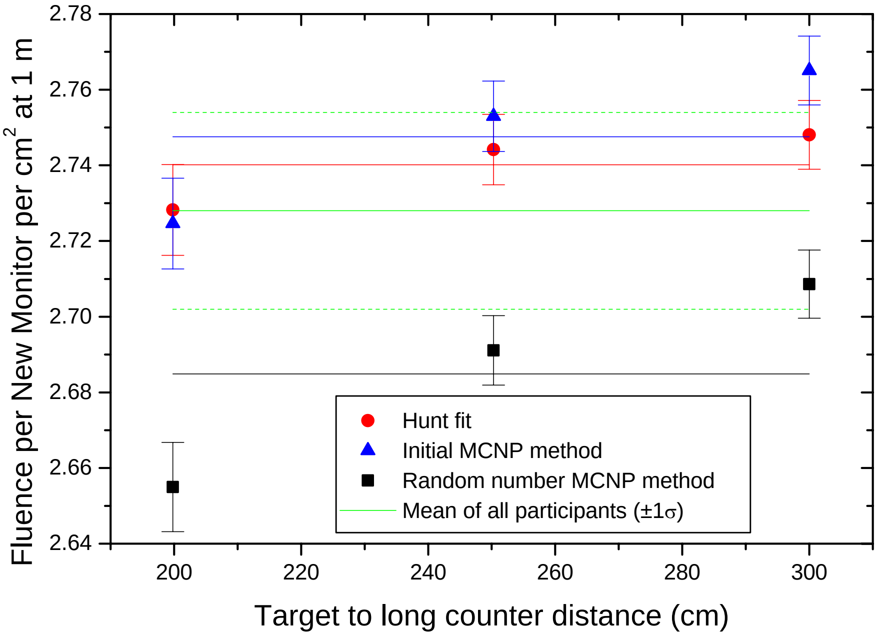

Figure 25: De Pangher 5.0 MeV fluence results using efficiencies and effective centres from Hunt's fit, the initial MCNP method and the random number MCNP method (solid lines represent mean values)

3.3.4 14.8 MeV

The De Pangher long counter is not routinely used at NPL for measuring fluence at 14.8 MeV. Aluminium activation foils form the standard at this energy. Therefore, for the intercomparison two such foils were irradiated and flown back to NPL to be β-counted. However, as the long counter was already in place it was decided to make measurements at 14.8 MeV to compare them with the foil results.

Table 15 gives the efficiency and effective centre values derived from the two calculational approaches and the fit of Hunt. The fluences obtained using the different effective centre values are shown in Figure 26, as well as the value derived from the foils. The Hunt effective centre is clearly too far into the long counter. The initial MCNP method value gives the best agreement with the aluminium foil result and the mean of all participants, although the random number MCNP method effective centre gives the most uniform values of fluence with target to long counter distance. This may indicate that the normalisation of the efficiency at this energy is not quite correct.

Overall, the performance of the De Pangher long counter at 14.8 MeV has been shown to be very good. Using the new effective centre and efficiency values, the measured values of the fluence agree with other standards laboratories and with activation foil measurements.

Table 15: Effective centre and efficiency values for the De Pangher long counter at 14.8 MeV

Method	Effective centre (cm)	Efficiency (cm^2)
Hunt fit	14.99	2.515
Initial MCNP	9.54	2.284
Random number MCNP	7.52	2.330

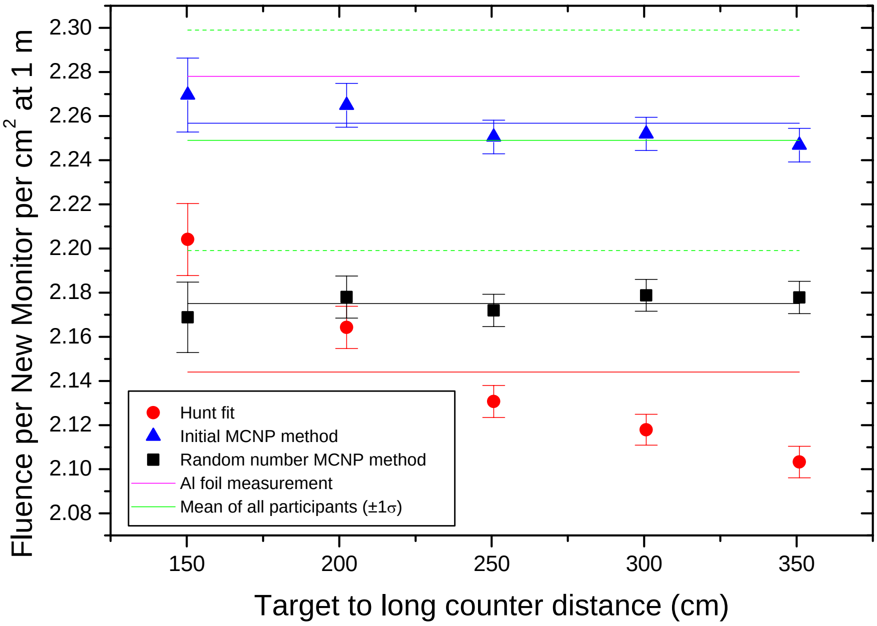

Figure 26: De Pangher 14.8 MeV fluence results using efficiencies and effective centres from Hunt's fit, the initial MCNP method and the random number MCNP method (solid lines represent mean values)

3.4 5″ Bonner sphere

As mentioned in section 2.6, the effective centre of a spherical device is conventionally taken as being at the centre of the sphere. To test this assumption, and to study the method of measuring effective centres, measurements were made with a 5″ Bonner sphere in the same way as measurements are made with the long counters.

The source used was a 555 GBq (15 Ci) ^{241}Am-Be source in an X14 capsule (serial number 1999NE) which is a cylinder 6 cm long by 3 cm in diameter. Using a source of this size (rather than an X3 which is 3.1 cm long by 2.2 cm diameter) was necessary to speed up the measurements at the further out distances. However, the physical size of the source meant that a large angle shadow cone (#7) had to be used for all positions and this led to overshadowing at the further distances.

The experiment gave an effective centre of (2.41 ± 0.78) cm. This disagrees with both the expected and the MCNP result. MCNP modelling of the NPL low scatter facility by Taylor[Ta97b] showed that the measured scatter component for area survey instruments using the shadow cone technique is underestimated by (5 ± 5)%. This is partly due to the shadow cone shielding a certain number of scattered neutrons in addition to the direct neutrons.

Sources of scatter shielded by the shadow cone include: material situated directly behind the source such as the Van de Graaff beam-lines, and air in-scatter from the penumbra region of the cone. In addition neutrons which pass through the detector and subsequently interact in the detector after having scattered off of the back wall are also excluded by the presence of the shadow cone.

For area survey meter calibrations with radionuclide neutron sources at NPL, 5% is added to the shadow cone readings to allow for the underestimation of the scatter component. A 5% component is also added in quadrature to the statistical shadow cone rate uncertainty. This approach was applied to the Bonner sphere readings which yielded an effective centre of (−3.09 ± 2.07) cm. This is 5.5 cm away from the effective centre value derived without the 5% additional scatter component, and the two values disagree by more than the size of the uncertainties.

In practice, the figure of 5% is only applicable to distances where calibrations are typically made (up to about 3 m from the source), and the degree of underestimation of scatter is less at positions further away from the source. A fit was therefore made only to the data points up to 3 m including the 5% additional scatter component. This gave an effective centre of (–0.21 ± 2.56) cm, which agrees with the expected value and also the MCNP calculated values.

As the fit to points up to 3 m gave the expected effective centre value, it was used to calculate the ‘true’ scatter-corrected values for each distance. These were then deducted from the measured total components to give the ‘true’ values of the scatter component for each distance. The ratios of these values to the actual measured scatter values were taken and are plotted in Figure 27. A linear fit was made to the points which shows a slight downward trend with distance suggesting that the underestimation of the scatter may be less as the detector moves further away from the source. This is perhaps a little surprising, as the degree of over-shadowing, i.e. the size of the umbra relative to the size of the detector, increases with distance. However, the uncertainties in the ratios are large and a flat line with a χ^2 value of 0.49 was also fitted to the points, indicating that the underestimation is (2.49 ± 0.34)% at each distance.

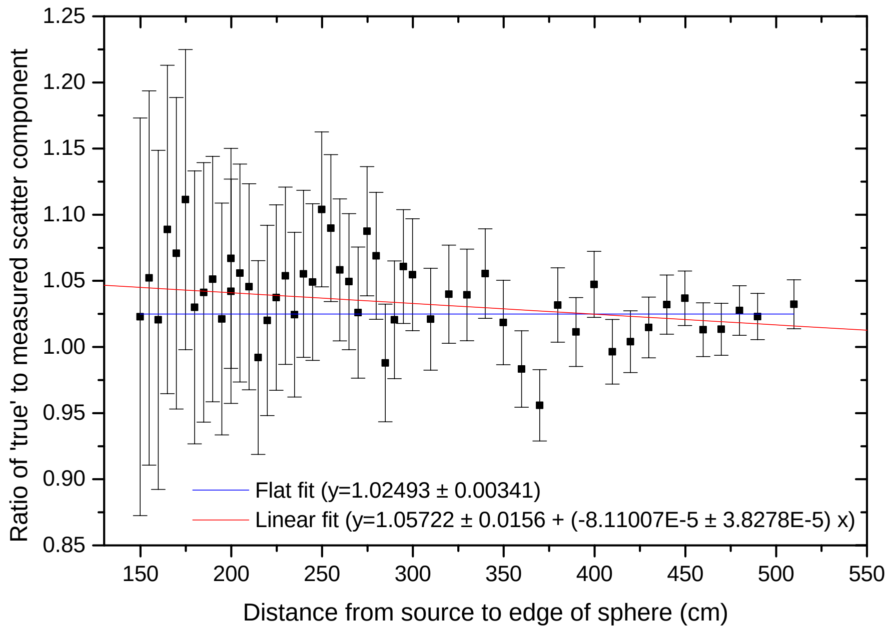

Figure 27: Ratio of 'true' to measured scatter components against distance for 5" Bonner sphere ^{241}Am-Be effective centre measurement

The measured scatter values were increased by 2.49% and their uncertainties had 2.49% added in quadrature to the statistical components. This yielded an effective centre of (–0.51 ± 1.26) cm which is in agreement with the expected value.

Perhaps the most important conclusion of the work with the 5″ sphere is that the value derived for the effective centre is very sensitive to the magnitude of the scatter component as measured with a shadow cone.

4 NORMALISATION OF EFFICIENCY CALCULATIONS

In light of new efficiency measurements for both long counters, it was appropriate to revisit the normalisation factors for the parallel beam MCNP calculations of Tagziria[Ta98]. Absolute normalisation of calculated efficiencies can be achieved using radionuclide sources calibrated in the NPL manganese bath, while monoenergetic measurements can be used to compare the ratios of the calculated responses of the two long counters with measurements.

4.1 Ratio of NPL long counter to De Pangher long counter monoenergetic response

Before the intercomparison exercise at PTB mentioned in section 3.3, a comparison of the NPL and De Pangher long counter responses for neutron energies of 144 keV, 2 MeV, and 5 MeV was performed at NPL. The results can be used to calculate the ratios of responses at each of the three energies. In order to do this, the measurements must be corrected to the same distance from the target (1 cm), which requires values for the effective centre to be used. In Table 16, the random number MCNP effective centre values have been used to make the distance correction for the measured responses.

Table 16: The ratios of the NPL to De Pangher long counter measured and calculated responses for 3 neutron energies

NPL to De Pangher ratio	144 keV	1.2 MeV	5 MeV
Measured response	3.530 ± 0.018	3.695 ± 0.021	3.727 ± 0.018
Parallel beam calculation (unnormalised)	3.177 ± 0.044	3.207 ± 0.045	3.339 ± 0.046
Measured/calculated	1.111 ± 0.016	1.152 ± 0.017	1.116 ± 0.016

Weighted mean NPL to De Pangher normalisation ratio = 1.125 ± 0.009[1]
(Uncertainty of weighted mean from spread of data = ± 0.013[2])

4.2 De Pangher long counter

Table 17 gives the ratios of measured to calculated efficiencies for the De Pangher long counter for a range of radionuclide sources. For ^{252}Cf, the measured efficiency from this work was used in preference to that of Tagziria due to the possibility that the ^{250}Cf component was not correctly allowed for in his analysis. The higher energy sources (^{252}Cf and ^{241}Am-Be) require a lower normalisation factor than the lower energy ones, although the weighted mean normalisation factor for all sources works out as unity. This demonstrates that the increase in the BF_3 density in the MCNP De Pangher model to normalise the calculations was correct.

Table 17: Calculated and measured De Pangher long counter efficiencies for radionuclide sources

Source	Present calculation (unnormalised)	Measurements This work	Measurements [Ta98][Ta01]	Measured /Calculated
^{124}Sb-Be	3.23 ± 0.04		3.24 ± 0.02	1.003 ± 0.014
^{241}Am-Li	3.40 ± 0.05	3.460 ± 0.042		1.017 ± 0.019
^{238}Pu-Li	3.38 ± 0.05		3.45 ± 0.02	1.021 ± 0.016
^{241}Am-F	3.46 ± 0.05		3.50 ± 0.04	1.012 ± 0.019
^{252}Cf	3.40 ± 0.05	3.313 ± 0.024	3.39 ± 0.02	0.974 ± 0.016
^{241}Am-Be	3.27 ± 0.04		3.22 ± 0.02	0.985 ± 0.014

Weighted mean normalisation factor = 1.000 ± 0.006
(Uncertainty from the spread of the data = ± 0.008)

No normalisation of the presently calculated efficiencies for the De Pangher long counter is therefore required. Hence, the normalised values calculated by Tagziria require no further normalisation. However, an uncertainty component of 0.7% should be added in quadrature to the overall uncertainty of 1.4% (from section 2.3.5.6) based on the standard error on the mean of the measured to calculated ratios for the six radionuclide sources. The final uncertainty in the calculated De Pangher long counter efficiency values is therefore ±1.6% at 1 sigma.

[1] Uncertainty, σ_m calculated from $\sigma_m^2 = 1/\sum w_i$ where $w_i = 1/\sigma_i^2$ and σ_i is the standard uncertainty in an individual measurement.

[2] Uncertainty from spread calculated using $\sigma_m^2 = \dfrac{\sum w_i (x_i - m)^2}{(n-1)\sum w_i}$ where *m* is the weighted mean value.

4.3 NPL long counter

Table 18 gives the ratios of measured to calculated efficiencies for the NPL long counter for the present calculations. For ^{252}Cf, the measured efficiency from this work was used in preference to that of Tagziria due to the possibility that the ^{250}Cf component was not correctly allowed for in his analysis. A weighted mean of the two measurements was used for ^{241}Am-Be. There is excellent agreement between the measured/calculated ratios for ^{241}Am-F, ^{252}Cf, and ^{241}Am-Be, but the ratios for the lower energy sources (^{124}Sb-Be, ^{241}Am-Li, and ^{238}Pu-Li) are 4.3 to 6.0% higher. This effect was noted earlier in section 3.2.1.3. The De Pangher ratios in Table 17 show the same effect but to a lesser degree. However, the monoenergetic results given in Table 16 do not show an increase in the NPL long counter efficiency at 144 keV, which is inconsistent with the radionuclide source results. This points to the neutron energy spectra used in the MCNP models, or the source measurements themselves as the cause of the discrepancy for the lower energy sources.

Table 18: Calculated and measured NPL long counter efficiencies for radionuclide sources

Source	Present calculation (unnormalised)	Measurements This work	Measurements [Ta98][Ta01]	Measured /Calculated
^{124}Sb-Be	9.70 ± 0.11		11.34 ± 0.07	1.169 ± 0.015
^{241}Am-Li	10.52 ± 0.14	12.34 ± 0.11		1.173 ± 0.019
^{238}Pu-Li	10.51 ± 0.14		12.49 ± 0.15	1.188 ± 0.021
^{241}Am-F	11.14 ± 0.15		12.49 ± 0.09	1.121 ± 0.017
^{252}Cf	10.96 ± 0.15	12.27 ± 0.11	12.51 ± 0.07	1.120 ± 0.018
^{241}Am-Be	10.80 ± 0.15	12.102 ± 0.088	12.12 ± 0.08	1.121 ± 0.017

Weighted mean normalisation factor = 1.147 ± 0.007
(Uncertainty from the spread of the data = ± 0.013)

Table 19 gives the NPL to De Pangher ratios of the measured/calculated responses for the six radionuclide sources. There is good agreement between the values with the exception of the ^{241}Am-F ratio. This could be because the neutron energy spectrum of this source, used in the MCNP model, is not very well defined.

Table 19: The ratios of the NPL to De Pangher long counter measured and calculated responses for radionuclide sources

Source	NPL to De Pangher Measured/Calculated Ratio
^{124}Sb-Be	1.165 ± 0.022
^{241}Am-Li	1.153 ± 0.029
^{238}Pu-Li	1.164 ± 0.028
^{241}Am-F	1.108 ± 0.027
^{252}Cf	1.149 ± 0.027
^{241}Am-Be	1.138 ± 0.024

Weighted mean NPL to De Pangher measured/calculated ratio = 1.147 ± 0.010
(Uncertainty from the spread of the data = ± 0.009)

The final normalisation factor for the NPL long counter efficiency calculations should take into account the monoenergetic comparison with the De Pangher long counter as well as the radionuclide source measurements. A weighted mean of the values given in Table 20 yielded the final normalisation factor. The monoenergetic ratio uncertainties had a 0.7% component added in quadrature to allow for the uncertainty in the De Pangher normalisation.

Table 20: Measured to calculated ratios for the NPL long counter for radionuclide and monoenergetic sources

Source	Measured/Calculated
^{124}Sb-Be	1.169 ± 0.015
^{241}Am-Li	1.173 ± 0.019
^{238}Pu-Li	1.188 ± 0.021
^{241}Am-F	1.121 ± 0.017
^{252}Cf	1.120 ± 0.018
^{241}Am-Be	1.121 ± 0.017
144 keV	1.111 ± 0.018
1.2 MeV	1.152 ± 0.019
5.0 MeV	1.116 ± 0.018

Weighted mean normalisation factor = 1.140 ± 0.006
(Uncertainty from the spread of the data = ± 0.010)

For the NPL long counter, a normalisation uncertainty component of 0.9% should be added in quadrature to the uncertainty of in the calculated efficiencies of 1.4% given in section 2.3.5.6. This comes from the standard error on the mean of the ratios given in Table 20. The overall uncertainty in the efficiency values for the NPL long counter is therefore ±1.7% at 1 sigma.

5 SENSITIVITY OF LONG COUNTER MEASUREMENTS TO OVERSHADOWING

In general, a Bonner sphere will be much more sensitive to scattered neutrons than a long counter. The response of a Bonner sphere with a spherical He-3 counter can be regarded as isotropic, whereas a long counter contains a thermal neutron absorbing layer of cadmium or boron to suppress neutrons incident from the rear and the sides. The ratio of scattered to total neutrons (the scatter fraction) for the 5″ Bonner sphere at 4.90 m from the ^{241}Am-Be source was 0.67 compared to only 0.25 for the NPL long counter at the same distance.

It could therefore be argued that the effect observed with the Bonner sphere (section 3.4) will not be applicable to the long counter, or at least not to the same degree. However, if the reason for the underestimation in the scatter measurement is that the cone shields scatter from material situated directly behind the source such as the Van de Graaff beam-lines, and/or air in-scatter from the penumbra region of the cone, then because these are incident on the front face of the long counter they would influence the long counter readings. Moreover, because the long counters are much more sensitive to neutrons incident on the front face the underestimation would have a greater relative impact on the scatter measurement than for the Bonner sphere.

The sensitivity of a long counter effective centre measurement to increases in the scatter measurement was investigated using the results from the De Pangher long counter ^{252}Cf and the NPL long counter ^{241}Am-Be measurements reported earlier in this report (sections 3.1.1.1 and 3.2.1.2). The same percentage increase was made to the shadow cone measured count rates at each distance. The magnitude of the increase was also added in quadrature to the statistical uncertainty for each scatter measurement.

The values of effective centre and efficiency obtained are plotted in Figure 28 and Figure 29. The variations of both are linear with the increase in the scatter component. For each 1 per cent increase in the scatter component for the NPL long counter measurement, the effective centre decreases by 0.24 cm and the efficiency decreases by 0.038 cm^2 (0.31%). For the De Pangher long counter measurement, the respective decreases in effective centre and efficiency are 0.25 cm and 0.011 cm^2 (0.33%).

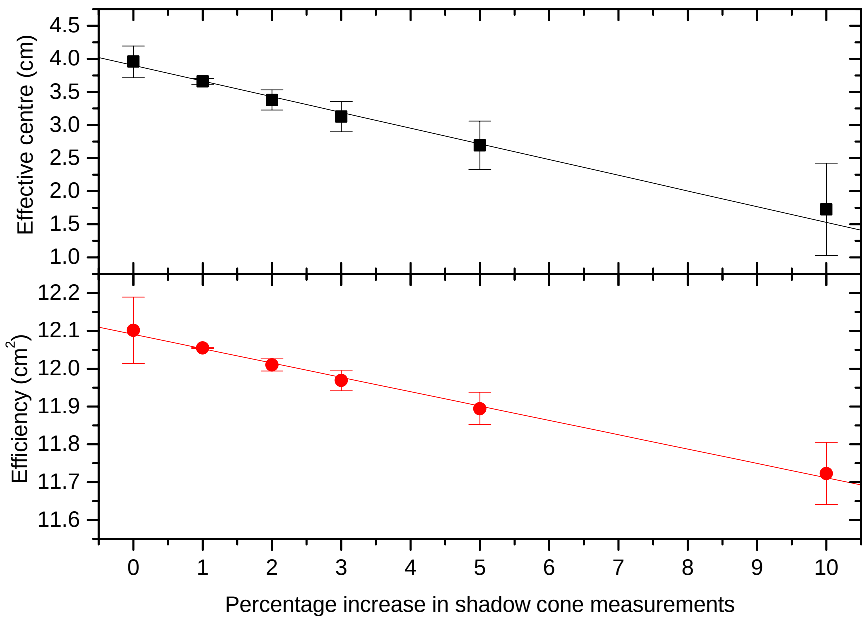

Figure 28: Change in effective centre (top) and efficiency (bottom) for percentage changes in scatter component for NPL long counter with a ^{241}Am-Be source (error bars for percentage increases >0 represent uncorrelated uncertainties)

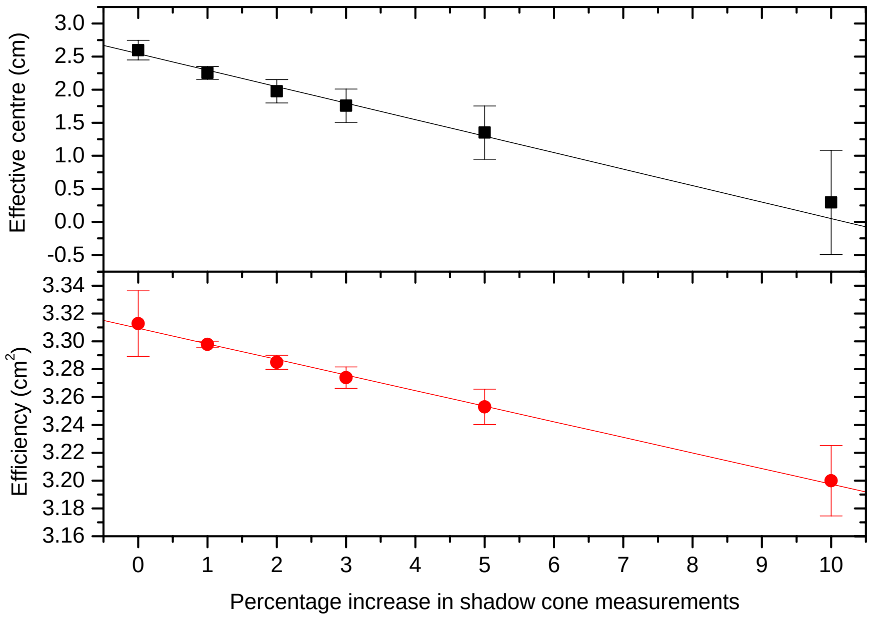

Figure 29: Change in effective centre (top) and efficiency (bottom) for percentage changes in scatter component for De Pangher long counter with a ^{252}Cf source (error bars for percentage increases >0 represent uncorrelated uncertainties)

Equations 2 and 6 can be combined to give the following relationship that should hold true for a particular distance when coupled values (i.e. values calculated or measured by the same method) for the efficiency and effective centre are used:

$$\frac{\varepsilon}{(r+r_o)^2} = \text{constant} \qquad (7)$$

By comparing the values from equation 7, the effects of changes in the effective centre and efficiency on a fluence measurement at a particular distance can be studied. Figure 30 shows the percentage change in measured fluence if the values for effective centre and efficiency are taken from the analysis with increased scatter components, compared to those with the measured scatter components for the De Pangher with a ^{252}Cf source.

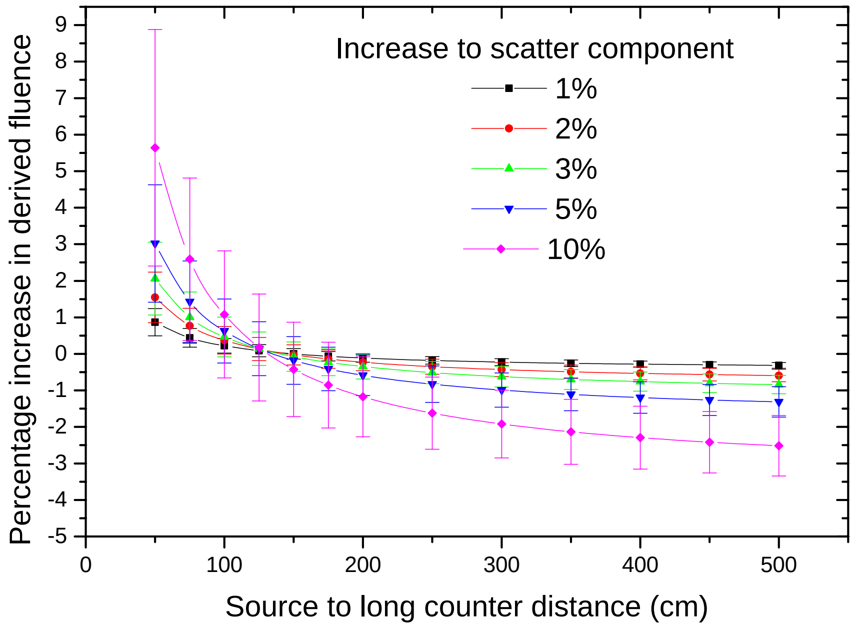

Figure 30: The percentage change in a fluence measurement for the values of effective centre and efficiency calculated using increased scatter components for the De Pangher long counter with a ^{252}Cf source (error bars represent uncorrelated uncertainties)

For the near points, the movement of the effective centre towards the front of the long counter has a greater effect on the measured fluence than the decrease in efficiency. But as r becomes greater, r_0 becomes less significant and the decrease in efficiency dominates. The two effects appear to cancel out at a distance of 125 cm, meaning that a fluence measurement at this point is independent of small changes in the scatter component during the effective centre and efficiency measurement.

6 CONCLUSION

This work has successfully produced reliable sets of effective centre and efficiency values for both long counters in use at NPL (see Appendices A & B). In addition to this, the sensitivity analysis has enabled justifiable uncertainties to be associated with the values calculated using MCNP. The aims of the project have therefore been achieved.

The evidence to support the new calculated values is in the form of new measurements performed at NPL with radionuclide sources and using the Van de Graaff accelerator to produce monoenergetic neutrons. The majority of previous measurements also validate the calculations in general. Most importantly, the CCRI intercomparison at PTB demonstrates the equivalence of fluence measurements made by NPL using the calculated effective centre and efficiency values with measurements made by other standards laboratories around the world.

The Monte Carlo code MCNP has also been used to further the understanding of the processes that give rise to the concept of an effective centre, and to investigate how the sensitivity of the De Pangher long counter varies across the front face.

There are some issues left unresolved such as the variability of measurements, and the variation in calculated efficiency normalisation factors for the NPL long counter that show a trend with energy. However, possible discrepancies in the calculated values have been allowed for in the uncertainties recommended here.

7 ACKNOWLEDGEMENTS

The authors would like to thank the following NPL staff: Sarb Cheema and John Sephton for designing and building the electronics required to automate the Pennine detector transport system, Lawrence Jones for assistance with measurements, Graeme Taylor for useful discussions on the subject of long counters, and Nigel Hawkes for proof-reading and commenting on this report.

This work was funded by the UK National Measurement System Policy Unit and was Deliverable (iv) of Project 3.2 in its 2001 to 2004 Programme for Ionising Radiation Monitoring Metrology. The title of the project was: *Determination of long counter effective centres.*

8 REFERENCES

[De66] J. De Pangher, and L.L. Nichols, *A Precision Long Counter for Measuring Fast Neutron Flux Density*, Pacific Northwest Laboratory Report BNWL-260, 1966.

[Ma70] T.O. Marshall, Some Tests on the Consistency of the Performance of Six Precision Long Counters Intended as Secondary Standards for the Measurement of Fast Neutron Flux Densities, Health Physics **18**, 427-429, 1970.

[Mc59] M.H. McTaggart, *A Study of the Neutron Long Counter*, AWRE report NR/A-1/59, 1959.

[Hu76] J.B. Hunt, *The Calibration and Use of Long Counters for the accurate measurement of Neutron Flux Density*, NPL Report RS(EXT)5, April 1976.

[Al60] W.D. Allen, *Fast Neutron Physics*, Part I, Chapter IIIA, Interscience publishers, New York, 1960.

[Br00] J.F. Briesmeister, editor, *MCNP™ - A General Monte Carlo N-Particle Transport Code, Version 4C*, edited by RSICC, Oak Ridge National Laboratory. LANL Manual LA-13709-M, March 2000

[Ta98] H. Tagziria and D.J. Thomas, *Re-calibration and Monte Carlo modelling of the NPL long counters*, NPL Report CIRM 19, September 1998.

[Ta01] H. Tagziria, N.J. Roberts, A. Bennett, and D.J. Thomas, *Calibration and Monte Carlo Modelling of the NPL Long Counters at 22.8 keV*, NPL Report CIRM 48, October 2001.

[Hu80] J.B. Hunt, K.G. Harrison, and R. Wilson, *Calibration of a De Pangher long counter and two neutron survey monitors at 21.5 keV*, Nuclear Instruments and Methods **169**, p477, 1980.

[IS00] International Organization for Standardization, ISO 8529-2:2000(E) *Reference neutron radiations, part 2*

[NI] http://physics.nist.gov/cgi-bin/Star/compos.pl?matno=213

[Ba01] D.T. Bartlett, R.J. Tanner, H. Tagziria, and D.J. Thomas, *Response Characteristics of Neutron Survey Instruments*, NRPB-R333*(rev)*, November 2001 (revised February 2002)

[Pen] Supplied by Pennine Automation Ltd. Brookwoods Industrial Estate, Holywell Green, Halifax, HX4 9BH, Tel. 01422 370109, http://www.pennineuk.com

[Ro01] N.J. Roberts, *MCNP Calculations of Correction Factors for Radionuclide Neutron Source Emission Rate Measurements using the Manganese Bath*, NPL Report CIRM 45, May 2001

[Th01] D.J. Thomas and N.J. Roberts, NPL, unpublished results.

[Hu72] J.B. Hunt, and J.C. Robertson, *The long counter as a secondary standard for neutron flux density*, In Proceedings of the 1st Symposium on Neutron Dosimetry in Biology and Medicine, Munich, 1972, Vol. II p935.

[Mo89] B. More, NPL, unpublished results.

[Th03] D.J. Thomas, NPL, unpublished results.

[Th91] D.J. Thomas, NPL, unpublished results.

[Hu89] J.B. Hunt, NPL, unpublished results.

[Ta97] G.C. Taylor, NPL, unpublished results.

[Th72] I.M.G Thomson, and A. Lavender, *Calibration of the De Pangher long counter,* in Neutron Monitoring for Radiation Protection Purposes, Proceedings of a Symposium, Vienna, 11-15 December 1972, Vol. II p483, Published by the IAEA, 1973.

[Ma72] O.P. Massand, *Investigation of Some Properties of the Precision Long Counter,* Report EUR 4783e, JNRC (now IRMM), JRC-EC, Geel, 1972.

[Mi72] B.J. Mijnheer, Standard Fluxes and Standard Moderating Counters for Neutron Fluence Measurements, IKO Amsterdam, Thesis, 1972

[He73] M. Heinzelmann, and F. Rohloff, *Das Effektive Zentrum des Long-Counters*, Nucl. Instrum. & Meths. **109**, 205, 1973.

[Ta99] G.C. Taylor, and N.J. Roberts, NPL, unpublished results.

[Th00] D.J. Thomas and N.J. Roberts, NPL, unpublished results.

[Sc98] D. Schlegel, *Target User's Manual,* PTB Laboratory Report PTB-6.41-1998-1, April 1998.

[Ta97b] G.C. Taylor, and D.J. Thomas, *Neutron scatter characteristics of the low-scatter facility of the Chadwick Building, NPL*, NPL Report CIRM 17, August 1998.

APPENDIX A: De Pangher long counter effective centre and efficiency values

Table A.1: De Pangher long counter effective centre and efficiency values calculated using MCNP with a point source at 50 different source to detector distances

Neutron energy (MeV)	Effective centre (cm)	Efficiency (cm^2)	Neutron energy (MeV)	Effective centre (cm)	Efficiency (cm^2)
0.001	1.12	3.560	2.150	3.92	3.532
0.020	1.27	3.294	2.200	3.70	3.530
0.070	1.23	3.256	2.500	4.06	3.515
0.100	0.82	3.240	2.700	4.05	3.434
0.120	0.69	3.215	2.814	3.51	3.213
0.144	0.95	3.220	2.815	3.23	2.981
0.180	1.13	3.273	2.816	4.18	3.268
0.475	1.70	3.371	2.830	3.88	3.326
0.565	2.12	3.403	2.900	3.63	3.228
0.700	2.42	3.438	2.950	3.35	3.147
1.000	2.72	3.490	2.975	4.11	3.378
1.100	2.54	3.371	3.000	4.58	3.531
1.130	2.54	3.494	3.100	3.99	3.391
1.170	2.66	3.500	3.200	4.22	3.294
1.190	2.66	3.501	3.300	4.06	3.221
1.200	2.72	3.507	3.500	4.06	3.134
1.210	2.86	3.511	3.600	3.74	3.130
1.230	2.91	3.512	4.000	4.40	3.221
1.250	2.86	3.390	4.400	4.63	3.341
1.260	3.09	3.517	4.650	5.29	3.354
1.300	3.10	3.526	5.000	5.85	3.363
1.400	3.09	3.524	5.200	5.76	3.339
1.600	3.00	3.529	6.000	5.89	3.232
1.900	3.48	3.542	14.800	7.52	2.293
2.040	3.73	3.528	15.535	7.66	2.250
2.070	3.59	3.338	16.010	7.78	2.224
2.078	2.33	2.972	17.000	7.81	2.145
2.090	3.16	3.438	18.971	7.68	2.040

Table A.2: De Pangher long counter efficiency values calculated using MCNP with a parallel beam

Neutron energy (MeV)	Efficiency (cm^2)
0.001	3.497
0.003	3.424
0.005	3.369
0.010	3.261
0.015	3.381
0.021	3.336
0.030	3.268
0.035	3.182
0.040	3.238
0.045	3.222
0.050	3.241
0.055	3.217
0.060	3.233
0.070	3.182
0.080	3.193
0.090	3.132
0.100	3.218
0.120	3.161
0.144	3.186
0.160	3.243
0.180	3.239
0.200	3.253
0.220	3.318
0.240	3.303
0.250	3.333
0.260	3.336
0.280	3.315
0.300	3.303
0.320	3.349
0.340	3.327
0.360	3.359
0.380	3.373
0.400	3.404
0.425	3.417
0.450	3.430
0.475	3.434
0.500	3.400
0.525	3.380
0.550	3.360
0.565	3.393
0.580	3.354
0.600	3.354
0.650	3.367
0.700	3.332
0.750	3.361
0.800	3.397
0.850	3.430
0.900	3.439
0.950	3.456
1.000	3.504
1.050	3.454
1.100	3.511
1.150	3.481
1.175	3.461
1.200	3.450
1.225	3.482
1.250	3.451
1.300	3.476
1.400	3.486
1.500	3.528
1.600	3.550
1.700	3.556
1.800	3.618
1.900	3.580
2.000	3.549
2.020	3.555
2.040	3.536
2.060	3.492
2.070	3.276
2.072	3.161
2.074	3.092
2.076	2.973
2.078	2.967
2.080	3.084
2.082	3.185
2.084	3.253
2.086	3.322
2.088	3.361
2.090	3.390
2.100	3.446
2.125	3.524
2.150	3.540
2.200	3.543
2.300	3.557
2.350	3.533
2.400	3.537
2.450	3.536
2.475	3.537
2.500	3.534
2.525	3.471
2.550	3.516
2.600	3.471
2.625	3.456
2.650	3.441
2.700	3.415
2.725	3.396
2.750	3.451
2.775	3.422
2.800	3.380
2.810	3.397
2.812	3.372
2.814	3.192
2.815	2.937
2.816	3.226
2.818	3.351
2.820	3.298
2.822	3.302
2.830	3.332
2.840	3.312
2.850	3.304
2.875	3.297
2.900	3.228
2.925	3.120
2.950	3.113
2.975	3.369
2.990	3.523
3.000	3.536
3.050	3.481
3.100	3.385
3.200	3.293
3.250	3.250
3.275	3.209
3.300	3.209
3.325	3.192
3.375	3.140
3.400	3.148
3.500	3.113
3.600	3.157
3.700	3.186
3.800	3.202
3.900	3.208
4.000	3.226
4.100	3.218
4.200	3.267
4.300	3.289
4.400	3.361
4.500	3.305
4.600	3.367
4.700	3.379
4.800	3.340
4.900	3.367
4.950	3.312
4.975	3.330
5.000	3.334
5.025	3.327
5.100	3.345
5.200	3.351
5.300	3.366
5.400	3.309
5.500	3.313
5.600	3.297
5.700	3.277
5.800	3.235
5.900	3.209
6.000	3.210
6.500	3.240
7.000	3.120
7.500	2.892
8.000	2.820
8.500	2.904
9.000	2.708
9.500	2.621
10.000	2.645
10.500	2.582
11.000	2.559
11.500	2.516
12.000	2.402
12.500	2.419
13.000	2.353
13.500	2.352
14.000	2.353
14.500	2.296
15.000	2.286
15.500	2.225
16.000	2.203

APPENDIX B: NPL long counter effective centre and efficiency values

Table B.1: NPL long counter effective centre and efficiency values calculated using MCNP with a point source at 50 different source to detector distances

Neutron energy (MeV)	Effective centre (cm)	Efficiency (cm^2)
0.030	-0.88	11.12
0.130	-0.81	11.37
0.144	-0.80	11.44
0.150	-0.86	11.50
0.525	-0.54	12.41
0.565	-0.54	12.42
0.570	-0.49	12.43
0.600	-0.22	12.47
0.800	0.36	12.60
1.100	0.82	12.70
1.200	0.86	12.73
1.300	0.96	12.76
1.600	1.10	12.98
2.000	1.57	13.03
2.040	1.57	12.99
2.076	-0.34	11.03
2.100	1.37	12.86
2.150	1.31	12.97
2.400	1.46	13.00
2.500	1.84	12.93
2.700	1.69	12.70
2.810	1.70	12.54

Neutron energy (MeV)	Effective centre (cm)	Efficiency (cm^2)
2.814	1.00	11.88
2.818	1.60	12.28
2.900	1.00	11.94
2.950	0.38	11.65
2.975	1.58	12.50
3.000	2.15	13.10
3.100	2.48	12.66
3.200	1.88	12.21
3.250	1.15	11.93
3.500	1.27	11.56
4.000	2.14	12.08
4.200	2.14	12.10
4.350	1.74	12.39
4.400	2.40	12.52
4.500	2.93	12.60
4.750	3.24	12.66
4.900	3.24	12.63
5.000	3.38	12.62
5.100	3.62	12.54
6.000	4.72	12.50
7.000	5.46	12.47

Table B.2: NPL long counter efficiency values calculated using MCNP with a parallel beam

Neutron energy (MeV)	Efficiency (cm^2)
0.001	11.51
0.003	11.34
0.005	11.32
0.010	11.20
0.015	11.05
0.021	11.16
0.025	11.10
0.030	11.01
0.035	11.35
0.040	11.35
0.045	10.97
0.050	11.17
0.055	11.12
0.060	11.03
0.065	11.26
0.070	11.31
0.075	11.29
0.080	11.34
0.085	11.26
0.090	11.28
0.095	11.34
0.100	11.42
0.110	11.43
0.120	11.45
0.130	11.24
0.140	11.40
0.150	11.57
0.160	11.57
0.170	11.52
0.180	11.63
0.190	11.51
0.200	11.55
0.250	11.69
0.260	11.69
0.270	11.82
0.280	11.75
0.300	11.79
0.320	11.82
0.340	11.85
0.350	11.84
0.360	11.85
0.380	11.88
0.400	11.88
0.425	11.92
0.450	12.17
0.475	12.20
0.500	12.26
0.525	12.42
0.565	12.38
0.580	12.32
0.600	12.48
0.650	12.47
0.700	12.54
0.750	12.54
0.800	12.42
0.850	12.61
0.900	12.72
1.000	12.68
1.050	12.76
1.175	12.76
1.200	12.68
1.225	12.79
1.250	12.85
1.300	12.87
1.350	12.89
1.400	12.93
1.450	13.01
1.500	13.00
1.550	12.92
1.600	12.95
1.650	12.69
1.700	13.02
1.750	13.00
1.800	12.98
1.850	12.90
1.900	12.89
1.950	12.95
2.000	13.01
2.020	13.00
2.040	12.94
2.060	12.76
2.070	12.24
2.072	11.93
2.074	11.50
2.076	11.00
2.078	11.04
2.080	11.51
2.082	11.86
2.084	12.20
2.086	12.40
2.088	12.55
2.090	12.57
2.100	12.66
2.150	12.92
2.200	12.92
2.250	13.01
2.300	12.96
2.350	12.89
2.450	12.92
2.475	12.94
2.500	12.79
2.525	12.74
2.550	12.78
2.600	12.75
2.650	12.81
2.700	12.57
2.750	12.55
2.775	12.49
2.800	12.51
2.810	12.58
2.812	12.48
2.814	11.80
2.816	11.99
2.818	12.36
2.820	12.33
2.822	12.31
2.830	12.33
2.840	12.28
2.850	12.22
2.875	12.18
2.900	12.11
2.925	11.71
2.950	11.62
2.975	12.45
2.990	12.97
3.000	13.19
3.050	12.90
3.100	12.65
3.150	12.45
3.200	12.22
3.250	12.07
3.300	11.87
3.350	11.81
3.400	11.65
3.450	11.63
3.500	11.53
3.550	11.62
3.600	11.58
3.650	11.59
3.700	11.66
3.750	11.63
3.800	11.73
3.850	11.84
3.900	11.90
3.950	11.93
4.000	12.10
4.150	12.12
4.200	12.11
4.250	12.23
4.300	12.34
4.350	12.33
4.400	11.51
4.500	12.54
4.550	12.61
4.600	12.61
4.650	12.61
4.700	12.64
4.750	12.93
4.800	12.75
4.850	12.62
4.900	12.59
4.950	12.60
4.975	12.61
5.000	12.67
5.025	12.79
5.050	12.69
5.100	12.69
5.150	12.70
5.200	12.86
5.250	12.81
5.300	12.64
5.350	12.65
5.400	12.57
5.450	12.64
5.500	12.73
5.600	12.76
5.700	12.69
5.800	12.67
5.900	12.51
6.000	12.46
6.500	12.76
8.000	11.12
8.500	11.75
9.000	10.89
9.500	10.74
10.000	10.81
10.500	10.72
11.000	10.81
11.500	10.52
12.000	10.39
12.500	10.13
13.000	10.04
13.500	10.12
14.000	9.97
14.500	9.91
15.000	9.81
15.500	9.72
16.000	9.53
17.000	9.34
17.500	9.31
18.000	9.09
18.500	9.18
19.000	8.94
19.500	8.98
20.000	8.91